Inorg. Chem. **2005**, *44*, 1511–1524

Structural Variations and Spectroscopic Properties of Luminescent Mono- and Multinuclear Silver(I) and Copper(I) Complexes Bearing Phosphine and Cyanide Ligands

Yong-Yue Lin,[†,‡] Siu-Wai Lai,*[,†] Chi-Ming Che,*[,†] Wen-Fu Fu,[†,‡] Zhong-Yuan Zhou,[§] and Nianyong Zhu[†]

Department of Chemistry and HKU-CAS Joint Laboratory on New Materials, The University of Hong Kong, Pokfulam Road, Hong Kong, Department of Chemistry, Yunnan Normal University, Kunming, 650092 Yunnan, P. R. China, and Department of Applied Biology and Chemical Technology, The Hong Kong Polytechnic University, Hunghom, Hong Kong

Received August 16, 2004

Reaction of equimolar amounts of AgCN and PCy_3 gave the polymer $[(Cy_3P)Ag(NCAgCN)]_\infty$ (**1**), whereas employment of excess PCy_3 yielded the discrete compound $[(Cy_3P)_2Ag(NCAgCN)]$ (**2**). Reacting bis(dicyclohexylphosphino)-methane (dcpm) with AgCN in 1:1 and 1:2 molar ratios gave two crystalline forms, namely $[Ag_2(\mu\text{-dcpm})_2][Ag(CN)_2]_2\cdot(CH_3OH)_2$ (**3a**·$(CH_3OH)_2$) and $[Ag_2(\mu\text{-dcpm})_2][Ag(CN)_2]_2$ (**3b**), respectively. The similar reaction of CuCN with PCy_3 afforded the polymeric compound $[\{(Cy_3P)Cu(CN)\}_3]_\infty$ (**4**), whereas treatment of CuCN with dcpm gave $[Cu_2(\mu\text{-dcpm})_2(CN)_2]$ (**5**). Employment of diphosphine ligands with longer $-(CH_2)_n-$ spacers, such as 1,2-bis-(dicyclohexylphosphino)ethane (dcpe, $n = 2$) and 1,3-bis(diphenylphosphino)propane (dppp, $n = 3$), in reactions with $[Cu(CH_3CN)_4]PF_6$ and KCN afforded the macrocylic compounds $[\{Cu(dcpe)\}_2(CN)(\mu\text{-dcpe})]PF_6$ (**6**(PF_6)) and $[\{Cu(dppp)\}_3(CN)_2(\mu\text{-dppp})]PF_6$ (**7**(PF_6)), respectively. The hexanuclear complex $[Cu(CN)(PCy_3)]_6$ (**8**) was obtained by reacting CuCN with PCy_3 in the presence of sodium pyridine-2-thiolate. The UV–vis absorption spectrum of **1** in acetonitrile displays a weak shoulder at 245 nm ($\epsilon = 350$ dm^3 mol^{-1} cm^{-1}). For **3a**, **3b**, and **5**, the intense absorption bands at $\lambda_{max} = 257$–276 nm with ϵ values of $(1.73–1.80) \times 10^4$ dm^3 mol^{-1} cm^{-1} are assigned to $[nd\sigma^* \rightarrow (n+1)p\sigma]$ transitions. Complexes **3a** and **3b** emit at $\lambda_{max} = 365$ nm in CH_3CN (quantum yield $\sim 6 \times 10^{-3}$, lifetime ~ 0.2 μs). The solid-state emission of **5** ($\lambda_{max} = 470$ and 488 nm at 298 and 77 K) is red-shifted in energy from that of **4** ($\lambda_{max} = 401$ and 405 nm at 298 and 77 K, respectively). In 77 K MeOH/EtOH (1:4) glassy solution, complexes **4**–**8** display intense emission with λ_{max} at 382–416 nm, which is assigned to the [3d → (4s, 4p)] triplet excited state.

Introduction

In the design and synthesis of molecular functional materials, transition-metal coordination using cyanometallate[1–3] and cyanide[4] as building blocks are becoming increasingly prevalent, and the judicious employment of ancillary ligands with different geometric constraints can afford supramolecular frameworks with diverse structures.[5,6] The structures and nuclearities of coordination polymers or molecular ensembles are often dictated by parameters such as stoichiometry of

* Authors to whom correspondence should be addressed. Email: cmche@hku.hk (C.M.C.); swlai@hku.hk (S.W.L.). Fax: +852 2857 1586 (C.M.C.).
† The University of Hong Kong.
‡ Yunnan Normal University.
§ The Hong Kong Polytechnic University.

(1) (a) Ouahab, L. *Chem. Mater.* **1997**, *9*, 1909−1926. (b) Ohba, M.; Okawa, H. *Coord. Chem. Rev.* **2000**, *198*, 313−328. (c) Moulton, B.; Zaworotko, M. J. *Chem. Rev.* **2001**, *101*, 1629−1658. (d) Niel, V.; Muñoz, M. C.; Gaspar, A. B.; Galet, A.; Levchenko, G.; Real, J. A. *Chem.—Eur. J.* **2002**, *8*, 2446−2453.

(2) (a) Soma, T.; Yuge, H.; Iwamoto, T. *Angew. Chem., Int. Ed. Engl.* **1994**, *33*, 1665−1666. (b) Soma, T.; Iwamoto, T. *Inorg. Chem.* **1996**, *35*, 1849−1856. (c) Černák, J.; Abboud, K. A.; Chomič, J.; Meisel, M. W.; Orendáč, M.; Orendáčová, A.; Feher, A. *Inorg. Chim. Acta* **2000**, *311*, 126−132. (d) Dasna, I.; Golhen, S.; Ouahab, L.; Daro, N.; Sutter, J.-P. *Polyhedron* **2001**, *20*, 1371−1374. (e) Černák, J.; Chomič, J.; Massa, W. *Acta Crystallogr., Sect. C* **2002**, *58*, m490−m493. (f) Dong, W.; Wang, Q.-L.; Si, S.-F.; Liao, D.-Z.; Jiang, Z.-H.; Yan, S.-P.; Cheng, P. *Inorg. Chem. Commun.* **2003**, *6*, 873−876. (g) Potočňák, I.; Triščíková, L.; Wagner, C. *Acta Crystallogr., Sect. C* **2003**, *59*, m249−m251.

(3) (a) Leznoff, D. B.; Xue, B.-Y.; Batchelor, R. J.; Einstein, F. W. B.; Patrick, B. O. *Inorg. Chem.* **2001**, *40*, 6026−6034. (b) Shorrock, C. J.; Xue, B.-Y.; Kim, P. B.; Batchelor, R. J.; Patrick, B. O.; Leznoff, D. B. *Inorg. Chem.* **2002**, *41*, 6743−6753. (c) White-Morris, R. L.; Stender, M.; Tinti, D. S.; Balch, A. L.; Rios, D.; Attar, S. *Inorg. Chem.* **2003**, *42*, 3237−3244.

10.1021/ic048876k CCC: $30.25
Published on Web 01/22/2005

reactants,[7,8] steric properties of ancillary ligands,[6,9] and presence of solvate or anion[9,10] during crystallization processes. Other subtle interactions, such as metallophilicity[3,11] and $\pi-\pi$ stacking,[12] may also play a role in controlling the supramolecular architecture.

In the context of increasing structural dimensionality and imparting intriguing photoluminescent characteristics to metal-containing assemblies, the employment of closed-shell d^{10} metal ions, including Cu(I), Ag(I), and Au(I), has long been demonstrated via weak metal−metal[13] and metal−ligand[14] interactions. The coordinatively unsaturated dicyanoaurates(I) and -argentates(I) are good candidates for examining $d^{10}-d^{10}$ interactions in the ground[15] and excited states,[16] and such interactions could lead to the formation of luminescent metal−metal-bonded excimers and metal−ligand exciplexes. For example, the two-coordinate $*Cu(CN)_2^-$, formed upon UV irradiation, was reported to associate with halide ions to give a long-lived, highly luminescent exciplex.[17]

Here we describe the structures of coordination polymers of Ag(I) and Cu(I) with cyanometallate or cyanide ions as bridging ligands and tricyclohexylphosphine (PCy_3) as the "capping" ligand. We also report the syntheses of di-, tri-, and hexanuclear assemblies with $[M_2(P^{\frown}P)_2]^{2+}$ (M = Cu and Ag; P$^{\frown}$P = bridging diphosphine), $[Cu_2(P^{\frown}P)(\mu\text{-}CN)]^+$, $[Cu_3(P^{\frown}P)(\mu\text{-}CN)_2]^+$, and $[Cu_6(\mu\text{-}CN)_6]$ core units, respectively. Their photophysical properties were examined, and comparisons with the respective mononuclear counterparts were made to probe and validate the presence and consequence of metal−metal interactions.

Experimental Section

General Procedures. All starting materials were used as received. $[Cu(CH_3CN)_4]PF_6$ was prepared by literature method.[18] Dichloromethane for photophysical studies was washed with concentrated sulfuric acid, 10% sodium hydrogen carbonate and water, dried by calcium chloride, and distilled over calcium hydride. Acetonitrile for photophysical measurements was distilled over potassium permanganate and calcium hydride. All other solvents were of analytical grade and purified according to conventional methods.[19] All reactions were carried out using standard Schlenk techniques with essential exclusion of light; for instance, reaction flasks were wrapped with opaque foil, filtration and evaporation were done under prevention of direct irradiation of light, recrystallization was carried out in the absence of light, and products were stored in amber glass vials with wrappings of opaque foil. Samples were dried under high vacuum prior to elemental analysis and NMR spectroscopic measurements.

Fast atom bombardment (FAB) mass spectra were obtained on a Finnigan Mat 95 mass spectrometer with a 3-nitrobenzyl alcohol matrix, whereas electrospray mass spectra were obtained on a LCQ quadrupole ion trap mass spectrometer. ^1H (500 MHz) and ^{31}P (202 MHz) NMR measurements were performed on a DPX 500 Bruker FT-NMR spectrometer with chemical shifts (in ppm) relative to tetramethylsilane (^1H) and H_3PO_4 (^{31}P) as references. Elemental analysis was performed by the Institute of Chemistry at the Chinese Academy of Sciences, Beijing. Infrared spectra were recorded on a Bio-Rad FT-IR spectrophotometer. UV−vis spectra were recorded on a Perkin−Elmer Lambda 19 UV/vis spectrophotometer.

Emission and Lifetime Measurements. Steady-state emission spectra were recorded on a SPEX 1681 Fluorolog-2 model F111AI spectrophotometer. Solution samples for measurements were degassed with at least four freeze−pump−thaw cycles. Low-temperature (77 K) emission spectra for glasses and solid-state samples were recorded in 5 mm diameter quartz tubes, which were placed in a liquid nitrogen Dewar equipped with quartz windows. The emission spectra were corrected for monochromator and photomultiplier efficiency and for xenon lamp stability.

Emission lifetime measurements were performed with a Quanta Ray DCR-3 pulsed Nd:YAG laser system (pulse output 266 nm, 8 ns). The emission signals were detected by a Hamamatsu R928 photomultiplier tube and recorded on a Tektronix TDS 350 oscilloscope. Errors for λ values (±1 nm), τ (±10%), Φ (±10%)

(4) (a) Chesnut, D. J.; Kusnetzow, A.; Zubieta, J. *J. Chem. Soc., Dalton Trans.* **1998**, 4081−4083. (b) Stocker, F. B.; Staeva, T. P.; Rienstra, C. M.; Britton, D. *Inorg. Chem.* **1999**, *38*, 984−991. (c) Darensbourg, D. J.; Lee, W.-Z.; Adams, M. J.; Larkins, D. L.; Reibenspies, J. H. *Inorg. Chem.* **1999**, *38*, 1378−1379. (d) Zhao, Y.; Hong, M.; Su, W.; Cao, R.; Zhou, Z.; Chan, A. S. C. *J. Chem. Soc., Dalton Trans.* **2000**, 1685−1686. (e) Liu, S.; Meyers, E. A.; Shore, S. G. *Angew. Chem., Int. Ed.* **2002**, *41*, 3609−3611. (f) Sun, X.-R.; Liang, J.-L.; Che, C.-M.; Zhu, N.; Zhang, X. X.; Gao, S. *Chem. Commun.* **2002**, 2090−2091.

(5) Iwamoto, T. In *Comprehensive Supramolecular Chemistry*; MacNicol, D. D., Toda, F., Bishop, R., Eds.; Pergamon Press: Oxford, 1996; Vol. 6, Chapter 19, pp 643−690.

(6) Blake, A. J.; Champness, N. R.; Hubberstey, P.; Li, W.-S.; Withersby, M. A.; Schröder, M. *Coord. Chem. Rev.* **1999**, *183*, 117−138.

(7) Bowmaker, G. A.; Effendy; Reid, J. C.; Rickard, C. E. F.; Skelton, B. W.; White, A. H. *J. Chem. Soc., Dalton Trans.* **1998**, 2139−2146.

(8) Marvaud, V.; Decroix, C.; Scuiller, A.; Tuyèras, F.; Guyard-Duhayon, C.; Vaissermann, J.; Marrot, J.; Gonnet, F.; Verdaguer, M. *Chem.−Eur. J.* **2003**, *9*, 1692−1705.

(9) (a) Chesnut, D. J.; Kusnetzow, A.; Birge, R.; Zubieta, J. *J. Chem. Soc., Dalton Trans.* **2001**, 2581−2586. (b) Bu, X.-H.; Xie, Y.-B.; Li, J.-R.; Zhang, R.-H. *Inorg. Chem.* **2003**, *42*, 7422−7430. (c) Song, R.-F.; Xie, Y.-B.; Li, J.-R.; Bu, X.-H. *J. Chem. Soc., Dalton Trans.* **2003**, 4742−4748.

(10) Withersby, M. A.; Blake, A. J.; Champness, N. R.; Hubberstey, P.; Li, W.-S.; Schröder, M. *Angew. Chem., Int. Ed. Engl.* **1997**, *36*, 2327−2329.

(11) (a) Shek, I. P. Y.; Wong, W.-Y.; Lau, T.-C. *New J. Chem.* **2000**, *24*, 733−734. (b) Leznoff, D. B.; Xue, B.-Y.; Patrick, B. O.; Sanchez, V.; Thompson, R. C. *Chem. Commun.* **2001**, 259−260.

(12) Blake, A. J.; Champness, N. R.; Khlobystov, A. N.; Lemenovskii, D. A.; Li, W.-S.; Schröder, M. *Chem. Commun.* **1997**, 1339−1340.

(13) (a) Jansen, M. *Angew. Chem., Int. Ed. Engl.* **1987**, *26*, 1098−1110. (b) Ford, P. C.; Vogler, A. *Acc. Chem. Res.* **1993**, *26*, 220−226. (c) Schmidbaur, H. *Chem. Soc. Rev.* **1995**, *24*, 391−400. (d) Pyykkö, P. *Chem. Rev.* **1997**, *97*, 597−636. (e) Puddephatt, R. J. *Chem. Commun.* **1998**, 1055−1062. (f) Patterson, H. H.; Kanan, S. M.; Omary, M. A. *Coord. Chem. Rev.* **2000**, *208*, 227−241.

(14) (a) Chan, W.-H.; Mak, T. C. W.; Che, C.-M. *J. Chem. Soc., Dalton Trans.* **1998**, 2275−2276. (b) Fu, W.-F.; Chan, K.-C.; Miskowski, V. M.; Che, C.-M. *Angew. Chem., Int. Ed.* **1999**, *38*, 2783−2785. (c) Che, C.-M.; Mao, Z.; Miskowski, V. M.; Tse, M.-C.; Chan, C.-K.; Cheung, K.-K.; Phillips, D. L.; Leung, K.-H. *Angew. Chem., Int. Ed.* **2000**, *39*, 4084−4088. (d) Fu, W.-F.; Chan, K.-C.; Cheung, K.-K.; Che, C.-M. *Chem.−Eur. J.* **2001**, *7*, 4656−4664. (e) Che, C.-M.; Lai, S.-W. *Coord. Chem. Rev.* in press.

(15) Rawashdeh-Omary, M. A.; Omary, M. A.; Patterson, H. H. *J. Am. Chem. Soc.* **2000**, *122*, 10371−10380.

(16) (a) Omary, M. A.; Patterson, H. H. *J. Am. Chem. Soc.* **1998**, *120*, 7696−7705. (b) Omary, M. A.; Patterson, H. H. *Inorg. Chem.* **1998**, *37*, 1060−1066. (c) Rawashdeh-Omary, M. A.; Omary, M. A.; Patterson, H. H.; Fackler, J. P., Jr. *J. Am. Chem. Soc.* **2001**, *123*, 11237−11247.

(17) (a) Horváth, A.; Stevenson, K. L. *Inorg. Chem.* **1993**, *32*, 2225−2227. (b) Horváth, A.; Wood, C. E.; Stevenson, K. L. *J. Phys. Chem.* **1994**, *98*, 6490−6495. (c) Horváth, A.; Wood, C. E.; Stevenson, K. L. *Inorg. Chem.* **1994**, *33*, 5351−5354. (d) Horváth, A. *Coord. Chem. Rev.* **1997**, *159*, 41−54. (e) Stevenson, K. L.; Jarboe, J. H. *J. Photochem. Photobiol., A* **2002**, *150*, 49−57.

(18) Kubas, G. J. *Inorg. Synth.* **1979**, *19*, 90−92.

(19) Perrin, D. D.; Armarego, W. L. F.; Perrin, D. R. *Purification of Laboratory Chemicals*, 2nd ed.; Pergamon: Oxford, 1980.

were estimated. The emission quantum yields were determined using the method of Demas and Crosby[20] with quinine sulfate in degassed 0.1 N sulfuric acid as a standard reference solution ($\Phi_r = 0.546$).

Synthesis. [(Cy$_3$P)Ag(NCAgCN)]$_\infty$, 1. To a stirred solution of tricyclohexylphosphine, PCy_3, (0.21 g, 0.75 mmol) in dichloromethane (30 mL) in the dark at 298 K was added AgCN (0.10 g, 0.75 mmol). The resultant suspension was refluxed under an argon atmosphere for 24 h, and the solution turned pale yellow. Upon cooling to room temperature, the mixture was filtered, and the volume of filtrate was reduced to ~5 mL. Addition of diethyl ether gave a white solid, which was collected by filtration and dried. Recrystallization by slow diffusion of diethyl ether into a dichloromethane solution gave colorless crystals: yield 0.12 g, 58%. Anal. Calcd for $C_{20}H_{33}N_2PAg_2$: C, 43.82; H, 6.07; N, 5.11. Found: C, 43.52; H, 6.16; N, 4.96. FAB-MS: *m/z* 387 $[(Cy_3P)Ag]^+$, 522 $[(Cy_3P)Ag_2(CN)]^+$, 670 $[(Cy_3P)(C)Ag_3(CN)_2]^+$, 683 $[(Cy_3P)Ag_3(CN)_3]^+$, 802 $[(Cy_3P)(C)Ag_4(CN)_3]^+$, 817 $[(Cy_3P)Ag_4(CN)_4]^+$, 937 $[(Cy_3P)(C)Ag_5(CN)_4]^+$, 1070 $[(Cy_3P)(C)Ag_6(CN)_5]^+$. ^{1}H NMR ($CDCl_3$): δ 1.19−1.35 (m, 15H, Cy), 1.73−1.76 (m, 3H, Cy), 1.86 (m, 15H, Cy). ^{31}P{^{1}H} NMR ($CDCl_3$): δ 41.15 (m, J [Ag^{107}−P] = 508 Hz, J [Ag^{109}−P] = 580 Hz). IR (KBr): ν 2154 (C≡N) cm^{-1}.

[(Cy$_3$P)$_2$Ag(NCAgCN)], 2. The procedure for **1** was adopted, except for using a 2:1 molar ratio of PCy_3 to AgCN, and a colorless crystalline solid was afforded: yield 0.19 g, 61%. Anal. Calcd for $C_{38}H_{66}N_2P_2Ag_2$: C, 55.08; H, 8.03; N, 3.38. Found: C, 55.14; H, 8.01; N, 2.87. FAB-MS: *m/z* 667 $[(Cy_3P)_2Ag]^+$, 802 $[(Cy_3P)_2Ag_2(CN)]^+$, 935 $[(Cy_3P)_2Ag_3(CN)_2]^+$, 1070 $[(Cy_3P)_2Ag_4(CN)_3]^+$, 1203 $[(Cy_3P)_2Ag_5(CN)_4]^+$. ^{1}H NMR ($CDCl_3$): δ 1.20−1.37 (m, 30H, Cy), 1.74−1.76 (m, 6H, Cy), 1.86 (m, 30H, Cy). ^{31}P{^{1}H} NMR ($CDCl_3$): δ 41.68 (m, J [Ag^{107}−P] = 524 Hz, J [Ag^{109}−P] = 598 Hz). IR (KBr): ν 2122 (C≡N) cm^{-1}.

[Ag$_2$(μ-dcpm)$_2$][Ag(CN)$_2$]$_2$·(CH$_3$OH)$_2$, 3a·(CH$_3$OH)$_2$. To a stirred solution of bis(dicyclohexylphosphino)methane, dcpm (0.42 g, 1.03 mmol), in dichloromethane (30 mL) in the dark at 298 K was added AgCN (0.14 g, 1.05 mmol). The resultant suspension was stirred under an argon atmosphere for 3 h, and the solution turned pale yellow. The mixture was filtered, and the volume of filtrate was reduced to ~5 mL; addition of diethyl ether gave a white solid, which was collected by filtration and dried. Recrystallization by slow diffusion of diethyl ether into a methanol/dichloromethane (1:3) solution yielded colorless crystals: yield 0.20 g, 57%. Anal. Calcd for $C_{54}H_{92}N_4P_4Ag_4$: C, 47.95; H, 6.85; N, 4.14. Found: C, 48.25; H, 6.89; N, 3.80. FAB-MS: *m/z* 1059 [$M^+ - Ag_2(CN)_3$], 1192 [$M^+ - Ag(CN)_2$], 1327 [$M^+ - CN$], 1461 [$M^+ + Ag$], 1595 [$M^+ + Ag_2(CN)$], 1728 [$M^+ + Ag_3(CN)_2$], 1863 [$M^+ + Ag_4(CN)_3$]. ^{1}H NMR ($CDCl_3$): δ 1.23−1.46 (m, 40H), 1.79 (m, 8H), 1.88−1.99 (m, 44H). ^{31}P{^{1}H} NMR ($CDCl_3$): δ 25.25 (d, J = 458 Hz). IR (KBr): ν 2102, 2135 (C≡N) cm^{-1}.

[Ag$_2$(μ-dcpm)$_2$][Ag(CN)$_2$]$_2$, 3b. The procedure for **3a·(CH$_3$OH)$_2$** was adopted using a 1:2 molar ratio of dcpm to AgCN and recrystallization by slow diffusion of diethyl ether into a dichloromethane solution, which afforded a colorless crystalline solid: yield 0.26 g, 74%. Anal. Calcd for $C_{54}H_{92}N_4P_4Ag_4$: C, 47.95; H, 6.85; N, 4.14. Found: C, 48.01; H, 7.06; N, 3.79. FAB-MS: *m/z* 1059 [$M^+ - Ag_2(CN)_3$], 1194 [$M^+ - Ag(CN)_2$], 1327 [$M^+ - CN$], 1460 [$M^+ + Ag$], 1595 [$M^+ + Ag_2(CN)$], 1728 [$M^+ + Ag_3(CN)_2$], 1861 [$M^+ + Ag_4(CN)_3$]. ^{1}H NMR ($CDCl_3$): δ 1.21−1.45 (m, 40H), 1.81 (m, 8H), 1.87−1.99 (m, 44H). ^{31}P{^{1}H} NMR ($CDCl_3$): δ 25.20 (d, J = 455 Hz). IR (KBr): ν 2140 (C≡N) cm^{-1}.

[{(Cy$_3$P)Cu(CN)}$_3$]$_\infty$, 4. To a stirred solution of PCy_3 (0.29 g, 1.03 mmol) in dichloromethane (30 mL) in the dark at 298 K was added CuCN (0.09 g, 1.00 mmol). The resultant suspension was refluxed under an argon atmosphere for 6 h and the solution turned pale green. Upon cooling to room temperature, the mixture was filtered, and the volume of filtrate was reduced to ~5 mL; addition of diethyl ether gave a white solid, which was collected by filtration and dried. Recrystallization by slow diffusion of diethyl ether into a dichloromethane solution afforded colorless crystals: yield 0.20 g, 54%. Anal. Calcd for $C_{57}H_{99}N_3P_3Cu_3$: C, 61.68; H, 8.99; N, 3.79. Found: C, 61.57; H, 9.01; N, 3.86. FAB-MS: *m/z* 624 $[(Cy_3P)_2Cu]^+$, 712 $[(Cy_3P)_2Cu_2(CN)]^+$, 803 $[(Cy_3P)_2Cu_3(CN)_2]^+$, 892 $[(Cy_3P)_2Cu_4(CN)_3]^+$, 981 $[(Cy_3P)_2Cu_5(CN)_4]^+$, 1072 $[(Cy_3P)_2Cu_6(CN)_5]^+$, 1161 $[(Cy_3P)_2Cu_7(CN)_6]^+$, 1250 $[(Cy_3P)_2Cu_8(CN)_7]^+$, 1341 $[(Cy_3P)_2Cu_9(CN)_8]^+$, 1430 $[(Cy_3P)_2Cu_{10}(CN)_9]^+$. ^{1}H NMR ($CDCl_3$): δ 1.21−1.46 (m, 45H), 1.72−1.93 (m, 54H). ^{31}P{^{1}H} NMR ($CDCl_3$): δ 12.99. IR (KBr): ν 2123 (C≡N) cm^{-1}.

[Cu$_2$(μ-dcpm)$_2$(CN)$_2$], 5. To a stirred solution of CuCN (0.045 g, 0.50 mmol) in dichloromethane (30 mL) was added dcpm (0.20 g, 0.49 mmol). The resultant suspension was refluxed under an argon atmosphere for 16 h. The mixture was cooled to room temperature and filtered, and the volume of the filtrate was reduced to ~5 mL. Addition of diethyl ether afforded a white precipitate, and recrystallization by diffusion of diethyl ether into a dichloromethane solution gave colorless crystals: yield 0.12 g, 48%. Anal. Calcd for $C_{52}H_{92}N_2P_4Cu_2$: C, 62.69; H, 9.31; N, 2.81. Found: C, 63.11; H, 9.58; N, 3.02. FAB-MS: *m/z* 560 $[(dcpm)Cu_2(CN)]^+$, 651 $[(dcpm)Cu_3(CN)_2]^+$, 740 $[(dcpm)Cu_4(CN)_3]^+$, 968 $[(dcpm)_2Cu_2(CN)]^+$, 1059 $[(dcpm)_2Cu_3(CN)_2]^+$, 1148 $[(dcpm)_2Cu_4(CN)_3]^+$. ^{1}H NMR ($CDCl_3$): δ 1.22−1.48 (m, 40H, Cy), 1.71−2.17 (m, 52H, Cy and CH_2). ^{31}P{^{1}H} NMR ($CDCl_3$): δ 6.46. IR (KBr): ν 2127 (C≡N) cm^{-1}.

[{Cu(dcpe)}$_2$(CN)(μ-dcpe)]PF$_6$, 6(PF$_6$). To a stirred solution of $[Cu(CH_3CN)_4]PF_6$ (0.18 g, 0.48 mmol) in methanol (15 mL) was added 1,2-bis(dicyclohexylphosphino)ethane, dcpe (0.31 g, 0.73 mmol). The white suspension was stirred until a clear solution was obtained. To this mixture was added KCN (41 mg, 0.63 mmol) to yield a white solid, which was dissolved upon addition of dichloromethane (10 mL) and stirred for 10 h at 298 K. The resultant white suspension was evaporated to dryness, and the solid was washed with a small amount of CH_2Cl_2 (~2 mL) and filtered. Recrystallization by slow diffusion of diethyl ether into a dichloromethane solution yielded colorless crystals: yield 0.14 g, 37%. Anal. Calcd for $C_{79}H_{144}NF_6P_7Cu_2$: C, 60.60; H, 9.27; N, 0.89. Found: C, 59.77; H, 9.15; N, 0.87. FAB-MS: *m/z* 998 $[(dcpe)_2Cu_2(CN)]^+$, 1088 $[(dcpe)_2Cu_3(CN)_2]^+$, 1177 $[(dcpe)_2Cu_4(CN)_3]^+$, 1268 $[(dcpe)_2Cu_5(CN)_4]^+$, 1357 $[(dcpe)_2Cu_6(CN)_5]^+$, 1447 $[(dcpe)_2Cu_7(CN)_6]^+$. ESI-MS: *m/z* 907.9 $[(dcpe)_2Cu]^+$, 998.5 $[(dcpe)_2Cu_2(CN)]^+$, 1420.0 [M^+], 1508.9 $[(dcpe)_3Cu_3(CN)_2]^+$. ^{1}H NMR ($CDCl_3$): δ 1.19−1.39 (m, 60H, Cy), 1.70−1.98 (m, 84H, Cy and CH_2). IR (Nujol): ν 2108 (C≡N) cm^{-1}. ^{31}P{^{1}H} NMR: See Results and Supporting Information.

[{Cu(dppp)}$_3$(CN)$_2$(μ-dppp)]PF$_6$, 7(PF$_6$). The procedure for **6**(PF_6) was adopted using 1,3-bis(diphenylphosphino)propane, dppp (0.27 g, 0.65 mmol), and recrystallization by slow diffusion of diethyl ether into an acetonitrile/dichloromethane (1:3) solution afforded colorless crystals: yield 0.11 g, 34%. Anal. Calcd for $C_{110}H_{104}N_2F_6P_9Cu_3$: C, 64.85; H, 5.14; N, 1.37. Found: C, 64.24; H, 5.15; N, 1.45. FAB-MS: *m/z* 978 $[(dppp)_2Cu_2(CN)]^+$, 1067 $[(dppp)_2Cu_3(CN)_2]^+$, 1156 $[(dppp)_2Cu_4(CN)_3]^+$, 1247 $[(dppp)_2Cu_5(CN)_4]^+$, 1336 $[(dppp)_2Cu_6(CN)_5]^+$, 1391 $[(dppp)_3Cu_2(CN)]^+$, 1480 $[(dppp)_3Cu_3(CN)_2]^+$, 1569 $[(dppp)_3Cu_4(CN)_3]^+$, 1892 [M^+]. ESI-MS: *m/z* 887.1 $[(dppp)_2Cu]^+$, 977.9 $[(dppp)_2Cu_2(CN)]^+$, 1068.6 $[(dppp)_2Cu_3(CN)_2]^+$, 1389.7 $[(dppp)_3Cu_2(CN)]^+$, 1478.7 $[(dppp)_3Cu_3$-

(20) Demas, J. N.; Crosby, G. A. *J. Phys. Chem.* **1971**, *75*, 991−1024.

$(CN)_2]^+$, 1892.5 [M^+]. ^{1}H NMR (CD_2Cl_2): δ 1.40−1.94 (m, 14H, CH_2), 2.31−2.43 (m, 10H, CH_2), 6.67−7.71 (m, 80H, Ph). IR (Nujol): ν 2116 (C≡N) cm^{-1}. ^{31}P{^{1}H} NMR: See Results and Supporting Information.

[Cu(CN)(PCy$_3$)]$_6$, 8. The procedure for $[Cu(CN)(PPh_3)_2]_6$[4d] was adopted using CuCN (0.046 g, 0.51 mmol), PCy_3 (0.28 g, 1.00 mmol), and sodium pyridine-2-thiolate (0.11 g, 0.83 mmol) to afford a pale-yellow solid: yield 0.12 g, 63%. Anal. Calcd for $C_{114}H_{198}N_6P_6Cu_6$: C, 61.68; H, 8.99; N, 3.79. Found: C, 60.89; H, 9.01; N, 3.72. FAB-MS: *m*/*z* 1072 $[(Cy_3P)_2Cu_6(CN)_5]^+$, 1161 $[(Cy_3P)_2Cu_7(CN)_6]^+$, 1250 $[(Cy_3P)_2Cu_8(CN)_7]^+$, 1341 $[(Cy_3P)_2Cu_9(CN)_8]^+$, 1430 $[(Cy_3P)_2Cu_{10}(CN)_9]^+$, 1519 $[(Cy_3P)_2Cu_{11}(CN)_{10}]^+$, 1608 $[(Cy_3P)_2Cu_{12}(CN)_{11}]^+$, 1699 $[(Cy_3P)_2Cu_{13}(CN)_{12}]^+$. ^{1}H NMR ($CDCl_3$): δ 1.20−1.40 (m, 90H), 1.71−1.88 (m, 108H). ^{31}P{^{1}H} NMR ($CDCl_3$): δ 12.17 (broad). IR (KBr): ν 2124 (C≡N) cm^{-1}.

X-ray Crystallography. Crystals of **1**−**8** were obtained by slow diffusion of diethyl ether into dichloromethane or CH_3OH/CH_2Cl_2 (1:3) or CH_3CN/CH_2Cl_2 (1:3) solutions. Crystal data and details of data collection and refinement are summarized in Table 1.

Data for complexes **2**, **3a**·$(CH_3OH)_2$, **3b**, and **4** were collected at 294 K on a Bruker CCD Area Detector diffractometer by the φ and ω scan technique using graphite-monochromated Mo Kα radiation (λ = 0.71073 Å). For these complexes, the coordinates of the metal atoms were determined by direct methods, and the remaining non-hydrogen atoms were located from successive Fourier difference syntheses. The structures were refined by full-matrix least-squares technique with anisotropic thermal parameters for all the non-hydrogen atoms. The calculations were performed on a COMPUCON PC/586 computer with the Bruker AXS SHELXTL/PC program package.[21] For **2**, a crystallographic asymmetric unit consists of one molecule. The crystallographic asymmetric units of **3a**·$(CH_3OH)_2$ and **3b** consist of half of one molecule, while the former contains one methanol molecule as solvent of crystallization. For **4**, a crystallographic asymmetric unit consists of one $[\{(Cy_3P)Cu(CN)\}_3]$ repeating group.

Diffraction experiments for **1**, **5**·$(CH_2Cl_2)_2$, **6**(PF_6)·Et_2O, **7**(PF_6)·0.5CH_3CN, and **8**·$(Et_2O)_2$ were performed at 301 K on an MAR diffractometer with graphite-monochromatized Mo Kα radiation (λ = 0.71073 Å). For **1**, the structure was solved by heavy-atom Patterson methods[22] and expanded using Fourier techniques.[23] Refinement of structures was performed by full-matrix least-squares technique using the software package TeXsan[24] on a Silicon Graphics Indy computer. The non-hydrogen atoms were refined anisotropically. Hydrogen atoms were included but not refined. The structures of **5**·$(CH_2Cl_2)_2$, **6**(PF_6)·Et_2O, **7**(PF_6)·0.5CH_3CN, and **8**·$(Et_2O)_2$ were solved by direct methods (SIR97),[25] and refinement of structures was performed by full-matrix least-squares technique using SHELXL-97[21] program package on a PC. For **1**, a crystallographic asymmetric unit consists of one formula unit. The structure is polymeric with Ag(2*) at $1-x$, $^1/_2+y$, $^1/_2-z$ bonded

Table 1. Crystal Data

	1	**2**	**3a**·$(CH_3OH)_2$	**3b**	**4**	**5**·$(CH_2Cl_2)_2$	**7**(PF_6)·0.5CH_3CN	**8**·$(Et_2O)_2$
formula	$C_{20}H_{33}N_2PAg_2$	$C_{38}H_{66}N_2P_2Ag_2$	$C_{56}H_{100}N_4O_2P_4Ag_4$	$C_{54}H_{92}N_4P_4Ag_4$	$C_{57}H_{99}N_3P_3Cu_3$	$C_{54}H_{96}N_2Cl_4P_4Cu_2$	$C_{111}H_{105.5}N_{2.5}F_6P_9Cu_3$	$C_{122}H_{218}N_6O_2P_6Cu_6$
fw	548.20	828.61	1416.76	1352.68	1109.92	1166.09	2057.83	2368.08
cryst size, mm^3	0.40 × 0.15 × 0.07	0.20 × 0.14 × 0.12	0.20 × 0.14 × 0.12	0.30 × 0.22 × 0.20	0.28 × 0.26 × 0. 20	0.40 × 0.20 ×0.10	0.50 × 0.30 ×0.20	0.40 × 0.20 ×0.20
cryst syst	orthorhombic	monoclinic	monoclinic	triclinic	triclinic	monoclinic	triclinic	triclinic
space group	$P2_12_12_1$ (No. 19)	$P2_1/n$	$P2_1/n$	$P\bar{1}$	$P\bar{1}$	$P2_1/c$	$P\bar{1}$	$P\bar{1}$
a, Å	9.943(2)	10.291(3)	12.027(3)	10.939(3)	11.456(3)	12.134(2)	13.621(3)	14.042(3)
b, Å	14.620(2)	29.554(8)	16.765(4)	12.686(3)	15.090(4)	10.847(2)	16.602(3)	14.550(3)
c, Å	15.259(3)	13.731(4)	15.996(4)	12.851(4)	18.440(4)	22.957(5)	25.019(5)	16.421(3)
α, deg	90	90	90	96.118(6)	94.674(6)	90	73.27(3)	100.43(3)
β, deg	90	107.169(7)	90.929(4)	113.275(5)	104.391(6)	91.31(3)	81.13(3)	102.39(3)
γ, deg	90	90	90	109.545(5)	101.276(5)	90	87.28(3)	93.84(3)
V, Å^3	2218.1(6)	3990.3(19)	3224.9(13)	1483.9(7)	2999.8 (12)	3020.8(10)	5353.4(19)	3203.1(11)
Z	4	4	2	1	2	2	2	1
D_c, g cm^{-3}	1.641	1.379	1.459	1.514	1.229	1.282	1.277	1.228
μ, mm^{-1}	1.838	1.088	1.335	1.445	1.170	1.022	0.782	1.101
$2\theta_{max}$, deg	51.2	55.14	55.12	55.12	55.20	50.94	50.70	50.70
no. unique data	2232	9198	7419	6734	13660	4899	14522	10118
no. obsd. data	2084 ($I > 3\sigma(I)$)	2876 ($I > 2\sigma(I)$)	4017 ($I > 2\sigma(I)$)	4416 ($I > 2\sigma(I)$)	4801 ($I > 2\sigma(I)$)	3468 ($I \geq 2\sigma(I)$)	8431 ($I \geq 2\sigma(I)$)	6728 ($I \geq 2\sigma(I)$)
R^a, R_w^b	0.028, 0.038	0.047, 0.064	0.050, 0.11	0.044, 0.084	0.064, 0.11	0.046, 0.12	0.063, 0.18	0.044, 0.13
residual ρ, eÅ^{-3}	+0.49, −0.52	+0.55, −0.76	+0.91, −0.91	+0.85, −0.62	+0.64, −0.35	+0.86, −0.41	+1.54, −0.53	+1.82, −0.68

^{a} $R = \sum||F_o| - |F_c||/\sum|F_o|$. ^{b} $R_w = [\sum w(|F_o| - |F_c|)^2/\sum w|F_o|^2]^{1/2}$.

(21) Sheldrick, G. M. *SHELX 97*, *Programs for Crystal Structure Analysis*; University of Göttingen: Göttingen, Germany, 1997.

(22) Beurskens, P. T.; Admiraal, G.; Beurskens, G.; Bosman, W. P.; Garcia-Granda, S.; Gould, R. O.; Smits, J. M. M.; Smykalla, C. *PATTY, The DIRDIF Program System: Technical Report of the Crystallography Laboratory*; University of Nijmegen: The Netherlands, 1992.

(23) Beurskens, P. T.; Admiraal, G.; Beurskens, G.; Bosman, W. P.; de Gelder, R.; Israel, R.; Smits, J. M. M. *The DIRDIF-94 Program System: Technical Report of the Crystallography Laboratory*; University of Nijmegen: The Netherlands, 1994.

(24) *TeXsan*: *Crystal Structure Analysis Package*; Molecular Structure Corporation: The Woodlands, Texas, 1985 and 1992.

(25) Altomare, A.; Burla, M. C.; Camalli, M.; Cascarano, M.; Giacovazzo, C.; Guagliardi, A.; Moliterni, A. G. G.; Polidori, G.; Spagna, R. *SIR97*. *J. Appl. Crystallogr*. **1998**, *32*, 115.

Scheme 1. Synthesis of **1**−**3a,b**

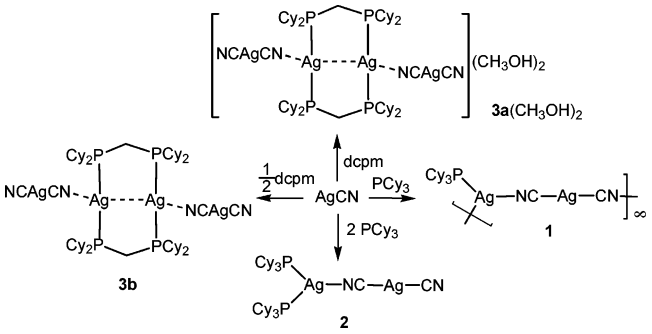

to C(1) and C(1*) at $1 - x$, $-^1/_2 + y$, $^1/_2 - z$ bonded to Ag(2) in the nearest neighborhood. For **5**·$(CH_2Cl_2)_2$, a crystallographic asymmetric unit consists of half of a formula unit, including one dichloromethane solvent molecule. All non-H atoms were refined anisotropically, and H atoms were generated by the SHELXL-97 program. For **6**(PF_6)·Et_2O, a crystallographic asymmetric unit consists of one formula unit with one diethyl ether molecule as solvent of crystallization. Only Cu, P, and cyanide were refined anisotropically, and other non-hydrogen atoms were located isotropically. The anion of PF_6^- was disordered by rotation along a F−P−F axis. The cyanide ligand was treated with disorder of C and N atoms. For **7**(PF_6)·$0.5CH_3CN$, one crystallographic asymmetric unit consists of one formula unit, including half of one acetonitrile solvent molecule and two halves of PF_6^- anions. Cyanide ligands were treated with disorder of C and N atoms. For **8**·$(Et_2O)_2$, one crystallographic asymmetric unit consists of half of a formula unit, including one diethyl ether solvent molecule.

Results

Synthesis and Characterization. Schemes 1 and 2 depict the synthesis of the silver (**1**−**3a**,**b**) and copper (**4**−**8**) compounds studied in this work. Reaction of AgCN and PCy_3 in equimolar ratio gave the coordination polymer $[(Cy_3P)Ag(NCAgCN)]_\infty$ (**1**). Upon altering the molar ratio of PCy_3:AgCN to 2:1, the discrete molecular complex $[(Cy_3P)_2Ag(NCAgCN)]$ (**2**) was afforded (Scheme 1). The $^{31}P\{^1H\}$ NMR spectrum of **1** displays doublets at δ 41.15 with J values of 508 and 580 Hz, whereas those of **2** appear at 41.68 ppm with J values of 524 and 598 Hz, which are due to $^1J(^{107}Ag-P)$ and $^1J(^{109}Ag-P)$ couplings, respectively. In the FT-IR spectra, the ν(C≡N) bands of **1** and **2** occur at 2154 and 2122 cm^{-1}, respectively. This is consistent with the less electrophilic nature of $[(Cy_3P)_2Ag]^+$ in **2** compared to that of $[(Cy_3P)Ag]^+$ in **1**, if we regard PCy_3 as a σ-donor. In comparison with ν(C≡N) of 2135 cm^{-1} in the free $[Ag(CN)_2]^-$ anion,[26] the higher ν(C≡N) stretching frequency in **1** suggests that the cyanoargentate ions in **1** behave as bridging linkages via both cyanide termini. The ancillary PCy_3 ligand plays a role in stabilizing the cyanometallate-directed polymeric structure of **1**.

In the literature, reactions of transition metal halides with bidentate phosphine ligands (P∩P), such as dppm or dcpm, in 1:1 stoichiometry were reported to afford compounds with the $[M_2(\mu\text{-P}\cap\text{P})_2]^{n+}$ framework (M = Re, Mo, Cu, Ag, Au, Pt, Mn).[27] In this work, reacting AgCN with dcpm in stoichiometric ratio of 1:1 and 2:1 gave **3a** and **3b**, respectively (Scheme 1), and both structures comprise the same $[Ag_2(\mu\text{-dcpm})_2]^{2+}$ core with minor structural deviations (see Scheme 1). The IR spectrum of **3a** displays two weak peaks at 2102 and 2135 cm^{-1}, which are consistent with two different cyanide coordination modes for the $[NCAgCN]^-$ units. The IR spectrum of **3b** shows one strong peak at 2140 cm^{-1}, indicating that the two cyanide groups are in a similar chemical environment without coordination to the $[Ag_2(\mu\text{-dcpm})_2]^{2+}$ core. The $^{31}P\{^1H\}$ NMR spectra of **3a** and **3b** show a similar broad doublet at ∼25.2 ppm with coupling constants (J) of ∼455 Hz. These silver(I) compounds (**1**−**3a,b**) are air-stable in the solid state, but they are stable in solution for a few days only in the absence of light.

Reaction of PCy_3 with CuCN in equal stoichiometry afforded the polymeric compound $[\{(Cy_3P)Cu(CN)\}_3]_\infty$ (**4**) (Scheme 2). The IR spectrum shows the ν(C≡N) stretching at 2123 cm^{-1}, which is comparable to that of 2122 cm^{-1} observed for **2**. In the $^{31}P\{^1H\}$ NMR spectrum of **4**, a peak is observed at 12.99 ppm that is significantly downfield from those of **1** and **2**, consistent with Cu(I) to be more electron rich than Ag(I). The discrete binuclear complex $[Cu_2(\mu\text{-dcpm})_2(CN)_2]$ (**5**) was obtained by reacting CuCN with dcpm in an equimolar ratio (Scheme 2), and the structure of the $[Cu_2(\mu\text{-dcpm})_2]^{2+}$ core is similar to that of $[Ag_2(\mu\text{-dcpm})_2]^{2+}$ in **3a** and **3b**. The employment of diphosphine ligands with longer $-(CH_2)_n-$ spacers, namely 1,2-bis(dicyclohexylphosphino)ethane (dcpe, $n = 2$) and 1,3-bis(diphenylphosphino)propane (dppp, $n = 3$), in reactions with $[Cu(CH_3CN)_4]PF_6$ followed by addition of KCN, afforded the ring compounds $[\{Cu(dcpe)\}_2(CN)(\mu\text{-dcpe})]PF_6$ (**6**(PF_6)) and $[\{Cu(dppp)\}_3(CN)_2(\mu\text{-dppp})]PF_6$ (**7**(PF_6)), respectively (Scheme 2). The hexanuclear compound $[Cu(CN)(PCy_3)]_6$ (**8**) was obtained by reacting CuCN with PCy_3 in the presence of sodium pyridine-2-thiolate (Scheme 2), a procedure similar to the preparation of $[Cu(CN)(PPh_3)_2]_6$.[4d] These copper(I) complexes (**4**−**8**) are air stable in solid and solution.

The IR spectra of **5**−**8** show ν(C≡N) stretchings in the 2108−2127 cm^{-1} range. The $^{31}P\{^1H\}$ NMR spectrum of **5** displays a peak at 6.46 ppm, whereas that of **6** shows broad signals in the range of −2.46 and 19.72 ppm. The $^{31}P\{^1H\}$ NMR spectrum of **7** in $CDCl_3$ at 40 °C shows two sets of three peaks as broad singlets at [−3.33, −11.03, −13.34 ppm] and [−8.19, −14.18, −17.27 ppm], respectively. The integration ratio for each set of three peaks is 1:2:1. In the $^{31}P\{^1H\}$ NMR spectrum of **7** at 20 °C, couplings were observed at signals with the chemical shift centered at −3.42 (broad triplet), −8.43 (triplet, $J = 47.4$ Hz), −10.98 (doublet, $J = 35.9$ Hz), and −14.29 ppm (doublet, $J = 46.0$ Hz). The $^{31}P-^{31}P$ COSY spectrum of **7** in CD_2Cl_2 at 25 °C shows cross peaks at the intersection of −3.50 ppm with −11.24

(26) Penneman, R. A.; Jones, L. H. *J. Inorg. Nucl. Chem.* **1961**, *20*, 19−31.

(27) (a) Brown, M. P.; Puddephatt, R. J.; Rashidi, M.; Seddon, K. R. *J. Chem. Soc., Dalton Trans.* **1978**, 1540−1544. (b) Benner, L. S.; Balch, A. L. *J. Am. Chem. Soc.* **1978**, *100*, 6099−6106. (c) Kubiak, C. P.; Woodcock, C.; Eisenberg, R. *Inorg. Chem.* **1980**, *19*, 2733−2739. (d) Kubiak, C. P.; Eisenberg, R. *J. Am. Chem. Soc.* **1980**, *102*, 3637−3639. (e) Frew, A. A.; Hill, R. H.; Manojlovic-Muir, L.; Muir, K. W.; Puddephatt, R. J. *J. Chem. Soc., Chem. Commun.* **1982**, 198−200.

Scheme 2. Synthesis of **4**−**8**

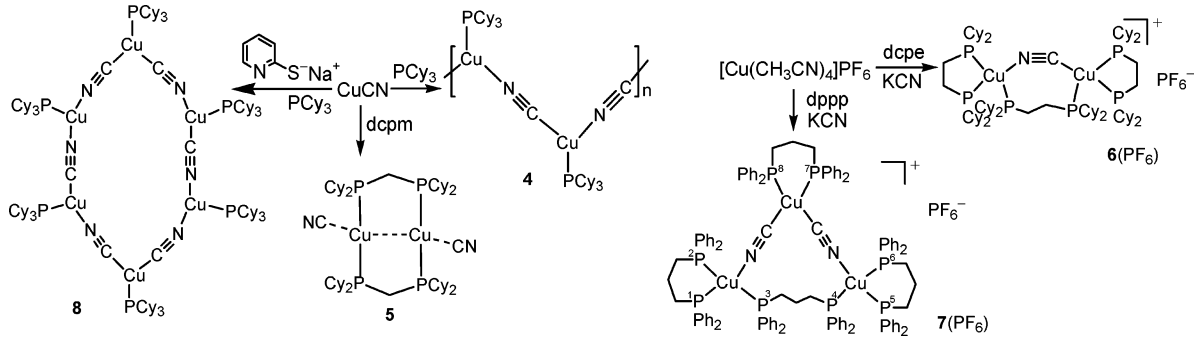

ppm and of −8.12 ppm with −14.43 ppm. This coupling connectivity, together with the multiplicity and integration ratio of peaks for **7**, suggests that two different structural conformers are in solution; there are two sets of three peaks in the $^{31}P\{^1H\}$ NMR spectrum of **7** [−3.42 ppm, broad t, P(3, 4); −10.98 ppm, d, J = 35.9 Hz, P(1, 2, 5, 6); −13.22 ppm, s, P(7, 8)] and [−8.43 ppm, t, J = 47.4 Hz, P(3, 4); −14.29 ppm, d, J = 46.0 Hz, P(1, 2, 5, 6); −17.30 ppm, s, P(7, 8)] (see Figures S2−S5 in the Supporting Information for details).

In the positive FAB mass spectra, peaks corresponding to cationic species with the formula of $[(Cy_3P)_2M_n(CN)_{n-1}]^+$ are apparent for **2** (M = Ag; n = 1−5), **4** (M = Cu; n = 1−10), and **8** (M = Cu; n = 6−13). Similarly, two cationic species with the formulas of $[(dcpm)Cu_n(CN)_{n-1}]^+$ and $[(dcpm)_2Cu_n(CN)_{n-1}]^+$ (n = 2−4) were detected in the mass spectrum of **5**, whereas for **6**, peaks attributable to the $[(dcpe)_2Cu_n(CN)_{n-1}]^+$ (n = 2−7) ions were observed. For **7**, the FAB mass spectrum shows the molecular ion at m/z 1892 as well as $[(dppp)_2Cu_n(CN)_{n-1}]^+$ (n = 2−6) and $[(dppp)_3Cu_n(CN)_{n-1}]^+$ (n = 2−4). The electrospray ionization mass spectra of **6** and **7** contain the molecular ion at m/z 1420.0 and 1892.5, respectively. The $[(L)_2Cu_n(CN)_{n-1}]^+$ (L = dcpe, n = 1−2 (for **6**); L = dppp, n = 1−3 (for **7**)) and $[(L)_3Cu_n(CN)_{n-1}]^+$ (L = dcpe, n = 3 (for **6**); L = dppp, n = 2−3 (for **7**)) species were also detected. These ionic clusters are commonly observed in the mass spectroscopy of metal−cyanide complexes.[28]

Crystal Structures. X-ray structural determinations of **1**, **2**, **3a**, **3b**, and **4**−**8** have been performed (Figures 1−8), and selected bond lengths and angles are listed in Table 2. The structure of **1** (Figure 1) consists of alternating $[(Cy_3P)Ag]^+$ units with μ-$[NCAgCN]^-$ cyanometallate linkers, forming a one-dimensional zigzag polymeric chain. The three-coordinate silver atoms of the $[(Cy_3P)Ag]^+$ units adopt a trigonal planar geometry and are coordinated to the linear $[NCAgCN]^-$ bridges. The bond angles at these silver atoms [P(1)−Ag(1)−N(1), N(1)−Ag(1)−N(2), and P(1)−Ag(1)−N(2)] lie in the range 100−136°, with the sum approaching 360°. The Ag−P bonds are coplanar with the plane defined by the $[Ag-NC-Ag-CN-]_n$ zigzag backbone. The mean Ag−N distance connecting $[(Cy_3P)Ag]^+$ units to $[NCAgCN]^-$ bridges is 2.24 Å, which is slightly longer than the Ag−C distances (mean 2.05 Å) in the $[Ag(CN)_2]^-$ unit. The $[NCAgCN]^-$ bridges two $[(Cy_3P)Ag]^+$ units with a span length of ∼10.8 Å and remains in a nearly linear geometry. Bending of the $(Cy_3P)Ag-N-C$ angle (157.2°) from linearity is observed upon coordination of $[NCAgCN]^-$ to $[(Cy_3P)Ag]^+$.

Complex $[(Cy_3P)_2Ag(NCAgCN)]$ (**2**) comprises a $[(Cy_3P)_2Ag]^+$ cation coordinated to $[NCAgCN]^-$ (Figure 2) to give a AgP_2N trigonal planar geometry. The Ag(1)−N(1) distance of 2.627(2) Å is longer than the corresponding Ag−N distances (mean 2.24 Å) in **1**. The mean Ag−C distance in $[NCAgCN]^-$ is 2.054 Å, which is comparable to the Ag−C distance of 2.153(6) Å in $[Ag(PCy_3)_2CN]$[29] and 2.15(6) Å in $[AgCN]_\infty$.[30] The $[Ag(CN)_2]^-$ ion is coordinated to $[(Cy_3P)_2Ag]^+$ with the C(37)−N(1)−Ag(1) angle of 171.1(2)°, whereas the geometry of the $[Ag(CN)_2]^-$ ligand remains close to linearity. The average Ag−P distance of 2.424 Å in **2** lies in the range of 2.333−2.429 Å reported for $[(PR_3)_2Ag]Cl$ (R = H, Me, tmpp)[31] and is slightly longer than that of 2.38 Å in **1**. This could be attributed to the steric effect because of the large cone angle (170°) of PCy_3[32] in comparison to that of 118, 137, and 145° for trimethyl-, triethyl-, and triphenylphosphine, respectively.

Crystals of **3a** were obtained with two methanol molecules per unit cell (Figure 3). The structure consists of a cationic $[Ag_2(\mu\text{-dcpm})_2]^{2+}$ core with two bridging dcpm ligands in a chair configuration; the P(2)−Ag(1)−P(1A) angle of 155.80(4)° shows significant deviation from linearity, and the P(2)−Ag(1)−Ag(1A) and P(1A)−Ag(1)−Ag(1A) angles are 92.33(3) and 87.83(3)°, respectively. Each of the silver atoms in $[Ag_2(\mu\text{-dcpm})_2]^{2+}$ is bound to $[NCAgCN]^-$ with an Ag−N distance of 2.452(4) Å. The N(1)−Ag(1)−Ag(1A) angle of 89.7(1)° is close to 90°, and the two $[NCAgCN]^-$ ions extend in opposite directions. The coordinated $[NCAgCN]^-$ anions remain close to linearity, whereas the C(25)−N(1)−Ag(1) angle of 153.8(4)° is bent. The intramolecular Ag···Ag distance of 2.8949(7) Å is comparable to those observed in polynuclear Ag(I) derivatives with proposed $d^{10}-d^{10}$ inter-

(28) (a) Jennings, K. R.; Kemp, T. J.; Sieklucka, B. *J. Chem. Soc., Dalton Trans.* **1988**, 2905−2911. (b) Dance, I. G.; Dean, P. A. W.; Fisher, K. J. *Inorg. Chem.* **1994**, *33*, 6261−6269. (c) Chu, I. K.; Shek, I. P. Y.; Siu, K. W. M.; Wong, W.-T.; Zuo, J.-L.; Lau, T.-C. *New J. Chem.* **2000**, *24*, 765−769. (d) Dance, I. G.; Dean, P. A. W.; Fisher, K. J.; Harris, H. H. *Inorg. Chem.* **2002**, *41*, 3560−3569.
(29) Bowmaker, G. A.; Effendy; Harvey, P. J.; Healy, P. C.; Skelton, B. W.; White, A. H. *J. Chem. Soc., Dalton Trans.* **1996**, 2449−2457.
(30) Bowmaker, G. A.; Kennedy, B. J.; Reid, J. C. *Inorg. Chem.* **1998**, *37*, 3968−3974.
(31) Bowmaker, G. A.; Schmidbaur, H.; Krüger, S.; Rösch, N. *Inorg. Chem.* **1997**, *36*, 1754−1757.
(32) Hormann-Arendt, A. L.; Shaw, C. F., III. *Inorg. Chem.* **1990**, *29*, 4683−4687.

Table 2. Selected Bond Lengths (Å) and Angles (deg)

complex **1**

Ag(1)−P(1)	2.380(1)	Ag(2)−C(2)	2.045(7)	Ag(1)−N(2)	2.207(5)	N(2)−C(2)	1.124(9)
Ag(1)−N(1)	2.263(5)	N(1)−C(1)	1.123(8)	Ag(2)−C(1)	2.047(6)		
N(1)−Ag(1)−N(2)	100.6(2)	Ag(2)−C(1)−N(1)	176.3(6)	P(1)−Ag(1)−N(2)	135.9(2)	Ag(2)−C(2)−N(2)	173.4(7)
P(1)−Ag(1)−N(1)	123.4(1)	Ag(1)−N(1)−C(1)	157.2(6)	C(1)−Ag(2)−C(2)	176.0(3)	Ag(1)−N(2)−C(2)	166.2(6)

complex **2**

Ag(1)−P(1)	2.4288(8)	Ag(2)−C(37)	2.051(3)	Ag(1)−N(1)	2.627(2)	N(2)−C(38)	1.152(3)
Ag(1)−P(2)	2.4196(8)	Ag(2)−C(38)	2.056(3)	N(1)−C(37)	1.115(3)		
P(2)−Ag(1)−P(1)	152.21(2)	N(1)−C(37)−Ag(2)	178.2(3)	P(2)−Ag(1)−N(1)	95.31(5)	N(2)−C(38)−Ag(2)	175.4(2)
P(1)−Ag(1)−N(1)	99.50(5)	C(37)−Ag(2)−C(38)	177.1(1)	C(37)−N(1)−Ag(1)	171.1(2)		

complex **3a**·$(CH_3OH)_2$

Ag(1)−Ag(1A)	2.8949(7)	Ag(1)−P(2)	2.408(1)	N(1)−C(25)	1.103(6)	P(1)−C(27)	1.827(4)	Ag(2)−C(25)	2.060(5)		
Ag(1)−P(1A)	2.422(1)	Ag(1)−N(1)	2.452(4)	Ag(2)−C(26)	2.029(6)	P(2)−C(27)	1.850(4)	N(2)−C(26)	1.142(7)		
P(2)−Ag(1)−P(1A)	155.80(4)	P(2)−Ag(1)−N(1)	107.5(1)	C(25)−N(1)−Ag(1)	153.8(4)	N(1)−Ag(1)−Ag(1A)	89.7(1)	P(1)−C(27)−P(2)	113.3(2)		
P(2)−Ag(1)−Ag(1A)	92.33(3)	C(27)−P(1)−Ag(1A)	108.7(1)	N(1)−C(25)−Ag(2)	172.5(5)	C(26)−Ag(2)−C(25)	179.9(3)				
P(1A)−Ag(1)−Ag(1A)	87.83(3)	C(27)−P(2)−Ag(1)	113.3(1)	P(1A)−Ag(1)−N(1)	96.8(1)	N(2)−C(26)−Ag(2)	178.4(8)				

complex **3b**

Ag(1)−Ag(1A)	2.9512(9)	Ag(1)−P(2A)	2.4125(9)	N(2)−C(27)	1.145(5)	P(1)−C(25)	1.839(3)	Ag(3)−C(27)	2.040(5)		
Ag(1)−P(1)	2.4087(9)	Ag(1)−N(1)	2.522(2)	Ag(2)−C(26)	2.052(3)	P(2)−C(25)	1.846(3)	C(26)−N(1)	1.139(4)		
P(1)−Ag(1)−P(2A)	158.95(2)	P(1)−Ag(1)−N(1)	102.91(7)	C(26)−N(1)−Ag(1)	140.1(2)	N(1)−Ag(1)−Ag(1A)	87.71(7)	P(1)−C(25)−P(2)	116.0(1)		
P(1)−Ag(1)−Ag(1A)	86.89(2)	C(25)−P(1)−Ag(1)	111.71(7)	N(1)−C(26)−Ag(2)	174.0(2)	C(27)−Ag(3)−C(27A)	180.000(1)				
P(2A)−Ag(1)−Ag(1A)	94.24(2)	C(25)−P(2)−Ag(1A)	111.58(9)	P(2A)−Ag(1)−N(1)	98.14(7)	N(2)−C(27)−Ag(3)	178.1(3)				

complex **4**

Cu(1)−C(55)	1.876(3)	Cu(2)−P(2)	2.264(1)	N(1)−C(55)	1.159(4)	Cu(3)−C(57)	1.866(3)
Cu(1)−N(3A)	1.945(4)	N(2)−C(56)	1.173(4)	Cu(2)−N(1)	1.950(3)	Cu(3)−P(3)	2.209(1)
Cu(1)−P(1)	2.243(1)	Cu(3)−N(2)	1.950(3)	Cu(2)−C(56)	1.870(4)	N(3)−C(57)	1.174(4)

C(55)−Cu(1)−N(3A)	116.4(1)	C(56)−Cu(2)−N(1)	125.4(1)	C(56)−N(2)−Cu(3)	166.4(3)	N(1)−Cu(2)−P(2)	113.14(9)	N(1)−C(55)−Cu(1)	174.2(4)		
C(55)−Cu(1)−P(1)	117.7(1)	N(2)−Cu(3)−P(3)	121.3(1)	C(57)−N(3)−Cu(1A)	175.2(3)	C(57)−Cu(3)−N(2)	106.9(1)	N(2)−C(56)−Cu(2)	172.9(3)		
N(3A)−Cu(1)−P(1)	125.66(9)	C(55)−N(1)−Cu(2)	170.3(3)	C(56)−Cu(2)−P(2)	121.3(1)	C(57)−Cu(3)−P(3)	131.7(1)	N(3)−C(57)−Cu(3)	169.7(3)		

complex **5**·$(CH_2Cl_2)_2$

Cu(1)−Cu(1*)	2.940(1)	P(2)−C(2)	1.844(4)	Cu(1)−P(1*)	2.263(1)	Cu(1)−C(1)	1.985(4)
Cu(1)−P(2)	2.262(1)	P(1)−C(2)	1.847(3)	P(1)−Cu(1*)	2.263(1)	N(1)−C(1)	1.101(5)

P(2)−Cu(1)−P(1*)	138.76(4)	C(1)−Cu(1)−P(2)	114.2(1)	N(1)−C(1)−Cu(1)	178.0(4)	C(1)−Cu(1)−Cu(1*)	104.9(1)	C(2)−P(2)−Cu(1)	111.2(1)		
C(1)−Cu(1)−P(1*)	106.9(1)	P(1*)−Cu(1)−Cu(1*)	82.58(3)	C(2)−P(1)−Cu(1*)	105.3(1)	P(2)−Cu(1)−Cu(1*)	90.33(3)	P(2)−C(2)−P(1)	113.6(2)		

Complex **6**(PF_6)·Et_2O

Cu(1)−N(1)	2.014(8)	Cu(1)−P(3)	2.412(3)	P(1)−C(1)	1.837(9)	P(3)−C(27)	1.870(9)	Cu(1)−P(2)	2.321(3)		
N(1)−C(1n)	1.15(1)	P(4)−C(28)	1.829(8)	C(1)−C(2)	1.56(1)	C(27)−C(28)	1.55(1)				
Cu(2)−C(1n)	1.998(8)	Cu(1)−P(1)	2.333(3)	Cu(2)−P(4)	2.473(3)	P(2)−C(2)	1.825(9)				
N(1)−Cu(1)−P(3)	95.1(2)	C(27)−P(3)−Cu(1)	108.6(3)	P(2)−Cu(1)−P(3)	120.6(1)	C(27)−C(28)−P(4)	114.2(6)	C(2)−P(2)−Cu(1)	104.7(3)		
C(1n)−N(1)−Cu(1)	158.1(7)	N(1)−Cu(1)−P(2)	115.2(2)	P(2)−Cu(1)−P(1)	88.79(9)	C(1)−P(1)−Cu(1)	101.5(3)				
N(1)−C(1n)−Cu(2)	161.2(7)	N(1)−Cu(1)−P(1)	114.6(2)	C(28)−P(4)−Cu(2)	106.6(3)	C(2)−C(1)−P(1)	110.2(6)				
C(1n)−Cu(2)−P(4)	96.4(2)	P(1)−Cu(1)−P(3)	124.5(1)	C(28)−C(27)−P(3)	114.3(6)	C(1)−C(2)−P(2)	112.8(6)				

complex **7**(PF_6)·$0.5CH_3CN$

Cu(1)−N(1)	1.985(7)	Cu(3)−C(2)	1.964(5)	Cu(1)−P(1)	2.285(2)	Cu(2)−P(4)	2.304(2)	P(2)−C(5)	1.847(6)		
Cu(1)−P(3)	2.308(2)	C(31)−C(32)	1.526(8)	P(1)−C(3)	1.832(7)	P(4)−C(32)	1.840(7)	Cu(1)−P(2)	2.300(2)		
N(1)−C(1)	1.129(8)	C(30)−C(31)	1.541(9)	N(2)−C(2)	1.147(8)	C(3)−C(4)	1.54(1)				
Cu(3)−C(1)	1.970(6)	P(3)−C(30)	1.834(6)	Cu(2)−N(2)	1.972(7)	C(4)−C(5)	1.53(1)				
N(1)−Cu(1)−P(3)	109.8(2)	N(2)−C(2)−Cu(3)	166.1(6)	P(1)−Cu(1)−P(2)	98.50(7)	C(32)−P(4)−Cu(2)	112.1(2)	C(4)−C(5)−P(2)	113.7(5)		
C(1)−N(1)−Cu(1)	167.1(6)	C(32)−C(31)−C(30)	111.7(5)	C(3)−P(1)−Cu(1)	107.7(2)	C(31)−C(32)−P(4)	110.4(4)	C(5)−P(2)−Cu(1)	113.5(2)		
N(1)−C(1)−Cu(3)	165.6(6)	C(31)−C(30)−P(3)	112.3(4)	C(2)−N(2)−Cu(2)	166.0(6)	C(4)−C(3)−P(1)	113.2(5)				
C(2)−Cu(3)−C(1)	100.8(2)	C(30)−P(3)−Cu(1)	114.6(2)	N(2)−Cu(2)−P(4)	108.5(2)	C(5)−C(4)−C(3)	114.2(6)				

complex **8**·$(Et_2O)_2$

Cu(1)−C(1)	1.918(5)	Cu(2)−C(3)	1.937(4)	Cu(1)−C(2)	1.931(5)	Cu(1)−P(1)	2.264(1)
N(1)−C(1)	1.140(5)	N(3)−C(3)	1.148(5)	N(2)−C(2)	1.156(5)	Cu(2)−P(2)	2.215(1)
Cu(3)−N(1)	1.933(4)	Cu(3)−N(3*)	1.922(5)	Cu(2)−N(2)	1.925(4)	Cu(3)−P(3)	2.255(1)

C(1)−Cu(1)−C(2)	128.9(2)	N(2)−C(2)−Cu(1)	176.5(4)	N(3*)−Cu(3)−N(1)	124.4(2)	N(2)−Cu(2)−C(3)	106.1(2)	N(3*)−Cu(3)−P(3)	128.2(1)		
C(1)−Cu(1)−P(1)	124.2(1)	N(3)−C(3)−Cu(2)	162.2(4)	N(1)−Cu(3)−P(3)	107.3(1)	N(2)−Cu(2)−P(2)	133.4(1)	N(1)−C(1)−Cu(1)	176.7(4)		
C(2)−Cu(1)−P(1)	106.9(1)	C(3)−N(3)−Cu(3*)	173.2(4)	C(2)−N(2)−Cu(2)	170.1(4)	C(3)−Cu(2)−P(2)	120.1(1)	C(1)−N(1)−Cu(3)	168.3(4)		

actions[33] and in $[Ag_2(dcpm)_2]X_2$ ($X = CF_3SO_3^-$, PF_6^-)[34] solids, and the latter were found by spectroscopic means to exhibit weak Ag−Ag interactions.

The molecular structure of **3b** shows virtually the same $[Ag_2(\mu\text{-dcpm})_2]^{2+}$ core with chairlike $[Ag_2P_4C_2]$ conformation (Figure S1 in the Supporting Information) as that observed

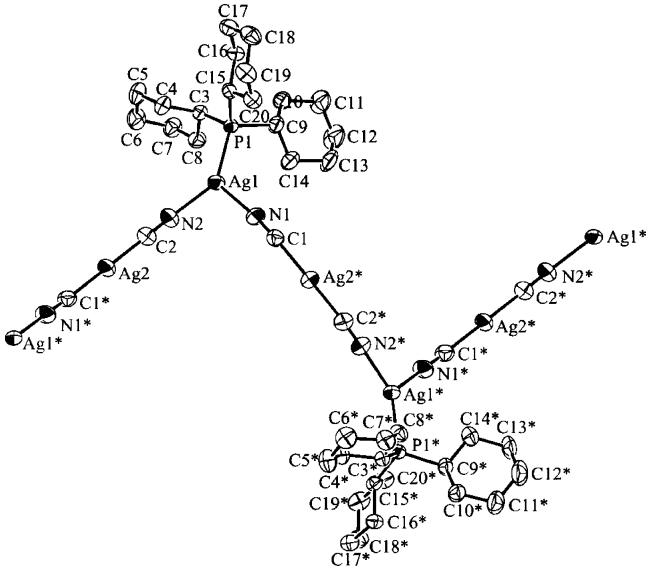

Figure 1. Perspective view of $[(Cy_3P)Ag(NCAgCN)]_\infty$, **1** (30% probability ellipsoids).

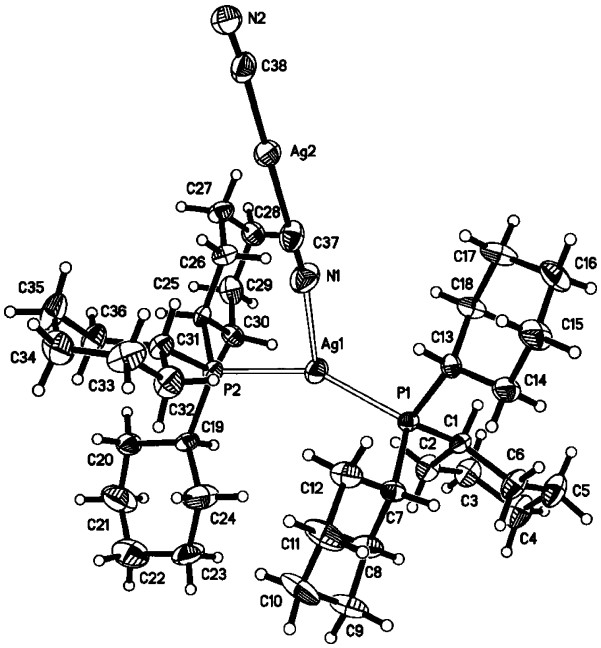

Figure 2. Perspective view of $[(Cy_3P)_2Ag(NCAgCN)]$, **2** (30% probability ellipsoids).

for **3a**·$(CH_3OH)_2$. The intramolecular Ag···Ag separation in **3b** (2.9512(9) Å) is slightly longer than that of 2.8949(7) Å in **3a**·$(CH_3OH)_2$, whereas the Ag−N(NCAgCN) distance of

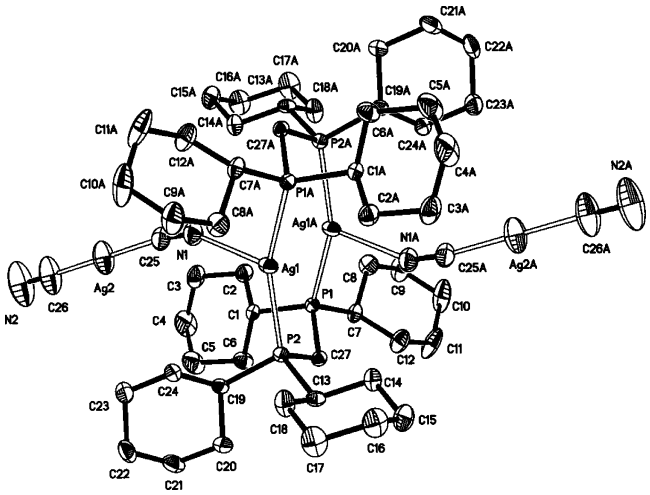

Figure 3. Perspective view of $[Ag_2(\mu\text{-dcpm})_2][Ag(CN)_2]_2$·$(CH_3OH)_2$, **3a**·$(CH_3OH)_2$ (30% probability ellipsoids).

2.522(2) Å in **3b** is also lengthened. The two $[NCAgCN]^-$ units are approximately perpendicular to the Ag···Ag vector.

The crystal structure of **4** consists of infinite one-dimensional $[(Cy_3P)Cu(CN)]_\infty$ zigzag chains with cyanide as a bridging ligand for $[Cu(PCy_3)]^+$ moieties (Figure 4). Similar Cu(CN) chains in the tetrahedral copper(I) diimine polymer $[Cu(dmphen)(CN)]_n$ (dmphen = 2,9-dimethyl-1,10-phenanthroline)[35] were previously reported. Each copper atom in **4** adopts a distorted trigonal planar geometry; the mean C−Cu−N, N−Cu−P, and C−Cu−P angles are 116.2, 120.0, and 123.6°, respectively. The average Cu−P (2.24 Å), Cu−C (1.87 Å), Cu−N (1.95 Å), and C−N (1.17 Å) distances agree well with those observed in the related complexes $[Cu(CN)(PPh_3)_2]_6$ (Cu−C 1.99 Å, Cu−N 2.02 Å, C−N 1.16 Å)[4d] and $[(CO)_5MCNCu(PPh_3)_3]$ (M = Cr, W; Cu−N 1.998 Å, C−N 1.15 Å).[36] The bridging cyanide ligand exhibits a span length of ∼4.99 Å between $[Cu(PCy_3)]^+$ units, and the $[Cu-CN-Cu]^+$ moieties remain close to linearity.

The molecular structure of **5** (Figure 5) shows a cationic $[Cu_2(\mu\text{-dcpm})_2]^{2+}$ core that is similar to those of $[Ag_2(\mu\text{-dcpm})_2]^{2+}$ in **3a**·$(CH_3OH)_2$ and **3b** (Figure 3 and Figure S1, respectively). The two Cu(I) centers are bridged by two dcpm ligands forming a chairlike $[Cu_2P_4C_2]$ core, and each Cu(I) is further coordinated to a cyanide ligand to afford a Y-shaped trigonal CuP_2C configuration. This structure was previously observed in $[Cu_2(\mu\text{-dcpm})_2(CH_3CN)_2]X_2$ and $[Cu_2(\mu\text{-dcpm})_2]X_2$ (X = ClO_4^-, PF_6^-).[14c,37] The two CuCN units approach linearity with the N(1)−C(1)−Cu(1) angle of 178.0° and are almost perpendicular to the Cu···Cu vector (C(1)−Cu(1)−Cu(1*) 104.9(1)°). The intramolecular Cu···Cu distance of 2.940(1) Å is close to the limit for metal−metal interactions; it is longer than those of 2.773(1)−2.821(2) Å

(33) (a) Kim, Y.; Seff, K. *J. Am. Chem. Soc.* **1978**, *100*, 175−180. (b) Eastland, G. W.; Mazid, M. A.; Russell, D. R.; Symons, M. C. R. *J. Chem. Soc., Dalton Trans.* **1980**, 1682−1687. (c) Papasergio, R. I.; Raston, C. L.; White, A. H. *J. Chem. Soc., Chem. Commun.* **1984**, 612−613. (d) Kappenstein, C.; Ouali, A.; Guerin, M.; Černák, J.; Chomič, J. *Inorg. Chim. Acta* **1988**, *147*, 189−197. (e) Chen, X. M.; Mak, T. C. W. *J. Chem. Soc., Dalton Trans.* **1991**, 1219−1222. (f) Quirós, M. *Acta Crystallogr., Sect. C* **1994**, *50*, 1236−1239. (g) Singh, K.; Long, J. R.; Stavropoulos, P. *J. Am. Chem. Soc.* **1997**, *119*, 2942−2943. (h) Omary, M. A.; Webb, T. R.; Assefa, Z.; Shankle, G. E.; Patterson, H. H. *Inorg. Chem.* **1998**, *37*, 1380−1386. (i) Villanneau, R.; Proust, A.; Robert, F.; Gouzerh, P. *Chem. Commun.* **1998**, 1491−1492. (j) Zank, J.; Schier, A.; Schmidbaur, H. *J. Chem. Soc., Dalton Trans.* **1999**, 415−420.

(34) Che, C.-M.; Tse, M.-C.; Chan, M. C. W.; Cheung, K.-K.; Phillips, D. L.; Leung, K.-H. *J. Am. Chem. Soc.* **2000**, *122*, 2464−2468.

(35) Morpurgo, G. O.; Dessy, G.; Fares, V. *J. Chem. Soc., Dalton Trans.* **1984**, 785−791.

(36) Darensbourg, D. J.; Yoder, J. C.; Holtcamp, M. W.; Klausmeyer, K. K.; Reibenspies, J. H. *Inorg. Chem.* **1996**, *35*, 4764−4769.

(37) Mao, Z.; Chao, H.-Y.; Hui, Z.; Che, C.-M.; Fu, W.-F.; Cheung, K.-K.; Zhu, N. *Chem.—Eur. J.* **2003**, *9*, 2885−2894.

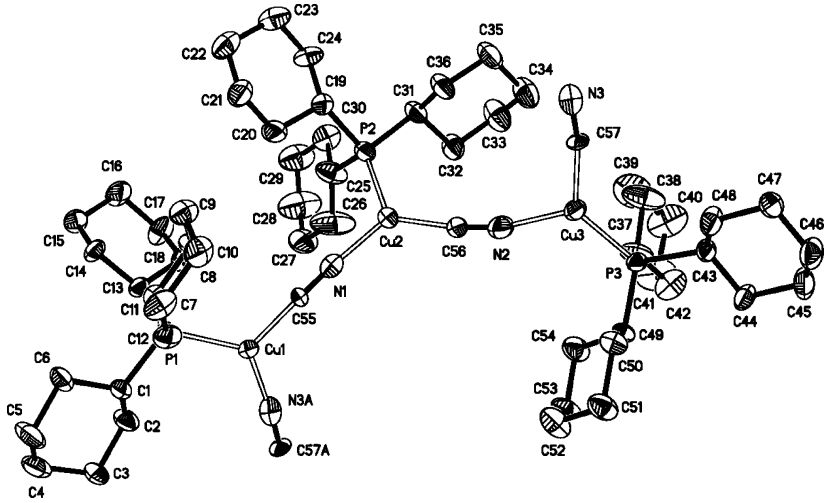

Figure 4. Perspective view of $[\{(Cy_3P)Cu(CN)\}_3]_\infty$, **4** (30% probability ellipsoids).

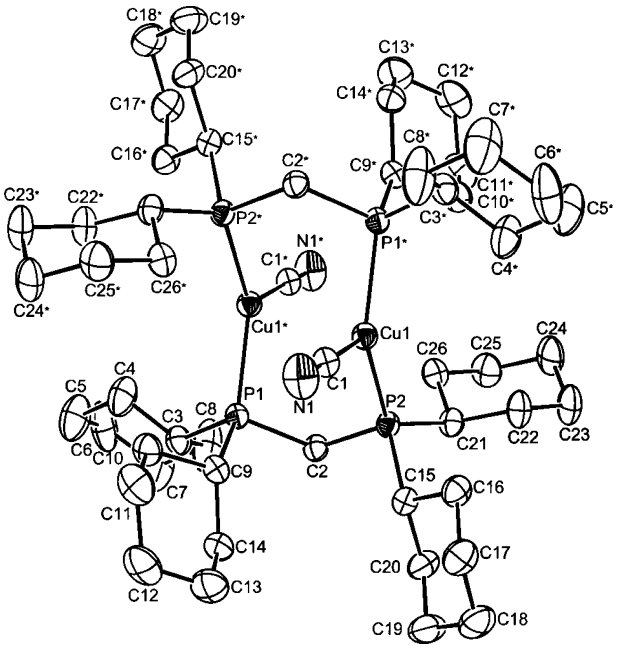

Figure 5. Perspective view of $[Cu_2(\mu\text{-dcpm})_2(CN)_2]$, **5** (30% probability ellipsoids).

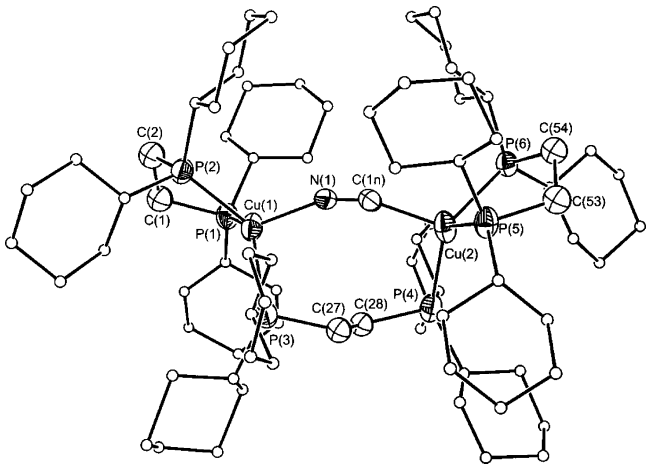

Figure 6. Perspective view of $[\{Cu(dcpe)\}_2(CN)(\mu\text{-dcpe})]PF_6$, **6**$(PF_6)$ (30% probability ellipsoids). The C atoms were drawn with small circles for clarity.

in $[Cu_2(\mu\text{-dcpm})_2X_2]$ ($X = I^-$, Cl^-, SCN^-).[14c,38] This can be rationalized by the stronger Cu(I)−CN interaction, which weakens the Cu(I)···Cu(I) interaction. The P(1*)−Cu(1)−P(2) angle (138.76(4)°) is comparable to those of 139.66(5)−145.25(5)° in the $[Cu_2(\mu\text{-dcpm})_2X_2]$ ($X = I^-$, Cl^-, SCN^-) complexes.[14c,38] The relatively large deviations of P−Cu−P angles from linearity further suggest that the CN^- ligands are engaged in strong interactions with Cu(I), comparable to that for the related $[Cu_2(\mu\text{-dcpm})_2I_2]$ complex.[14c,37]

As depicted in Figure 6, the two copper atoms in **6** are each chelated by a dcpe ligand to give five-membered $[Cu(dcpe)]^+$ moieties, and these are bridged by one cyanide linker and a dcpe ligand to afford the eight-membered $[Cu(CN)(dcpe)Cu]^+$ ring. The diameter of the core is estimated to be ∼5 Å, whereas the intramolecular Cu(1)···Cu(2) separation of 4.915 Å is excessively long for cuprophilic interaction. The C(1n)−N(1)−Cu(1) (158.1(7)°) and N(1)−C(1n)−Cu(2) (161.2(7)°) angles are significantly deviated from linearity. The copper atoms adopt a distorted tetrahedral coordination with the N−Cu−P and P−Cu−P angles lying in the range of 88.12(9)−125.6(1)°.

Figure 7 depicts the structure of **7**, which contains a trinuclear Cu(I) core. Each metal vertex comprises a six-membered $[Cu(dppp)]^+$ ring in a distorted chair configuration. One $[Cu(dppp)]^+$ group is coordinated to two cyanide ligands, each of which is further bound to another $[Cu(dppp)]^+$ unit. The Cu(1)···Cu(3) and Cu(2)···Cu(3) separations are 4.98 Å. Two $[Cu(dppp)]^+$ units are bridged by a dppp ligand, and the Cu(1)···Cu(2) distance is 6.83 Å. The mean C−N−Cu (166.6°) and N−C−Cu (165.9°) angles are slightly bent. The three copper atoms adopt a tetrahedral geometry, and the C(1)−Cu(3)−C(2), N(1)−Cu(1)−P(3), and N(2)−Cu(2)−P(4) angles are 100.8, 109.8, and 108.5°, respectively, suggesting minimal angle strain inside the 12-membered Cu_3 core.

The structure of $[Cu(CN)(PCy_3)]_6$ (**8**) features a hexagonal-like 18-membered ring with six three-coordinate copper

(38) Tse, M.-C. Ph.D. Thesis, The University of Hong Kong, 1999.

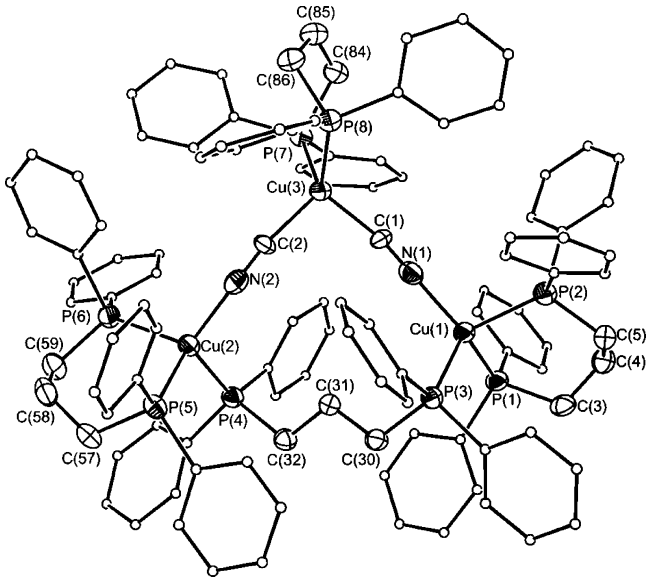

Figure 7. Perspective view of $[\{Cu(dppp)\}_3(CN)_2(\mu\text{-dppp})]PF_6$, **7**($PF_6$) (30% probability ellipsoids). The C atoms were drawn with small circles for clarity.

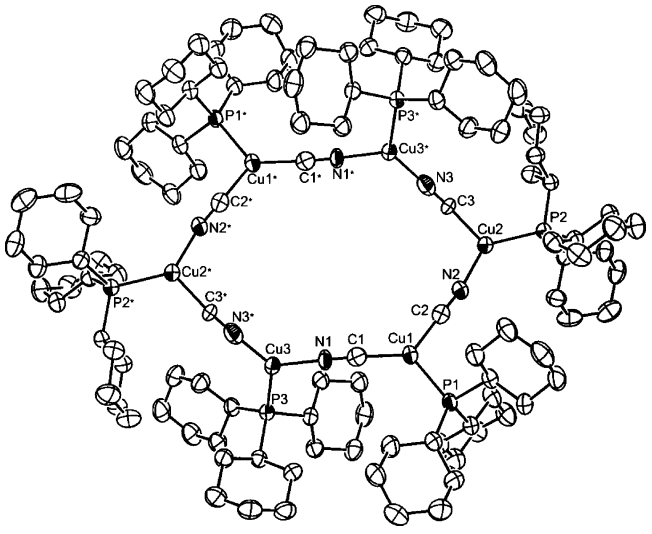

Figure 8. Perspective view of $[Cu(CN)(PCy_3)]_6$, **8** (30% probability ellipsoids).

vertexes in approximately trigonal planar geometry and bridged by six cyanide linkages (Figure 8). The structure is reminiscent of $[Cu(CN)(PPh_3)_2]_6$,[4d] except that each copper atom is coordinated to one PCy_3 ligand instead of two PPh_3 ligands in $[Cu(CN)(PPh_3)_2]_6$. The six cyanide linkers between the $[Cu(PCy_3)]^+$ vertexes constitute six sides of the hexagonal-like core, and the mean Cu···Cu separation is ~5 Å. The C−N−Cu and N−C−Cu angles (162.2−176.7°) slightly deviate from 180°, and indeed, the hexagonal core is nonplanar. The N(2)−Cu(2)−C(3) (106.1(2)°) angle shows a significant deviation from the 120° value expected for a hexagonal-shaped macrocycle, while the other C/N−Cu−C/N angles are ~124.4°. The distances between opposing copper atoms are 8.90, 11.50, and 8.68 Å. The dimensions of the central core are estimated to be 11.5 Å in length and 7.3 Å in width.

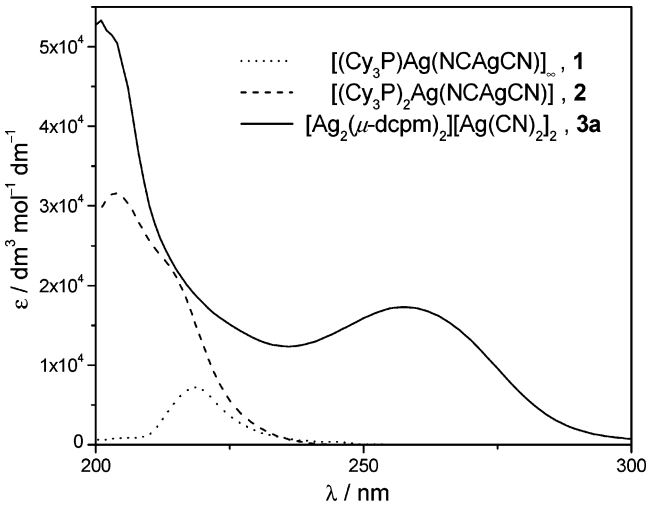

Figure 9. UV−vis absorption spectra of **1**, **2**, and **3a** in acetonitrile at 298 K.

Table 3. UV−Visible Absorption Data of Complexes **1**−**8**

complex	λ_{max}/nm (ϵ/dm^3 mol^{-1} cm^{-1})
$[(Cy_3P)Ag(NCAgCN)]_\infty$, **1**[a]	218 (7200), 245 (350)
$[(Cy_3P)_2Ag(NCAgCN)]$, **2**[a]	203 (31500), 216 (sh, 23000)
$[Ag_2(\mu\text{-dcpm})_2][Ag(CN)_2]_2$, **3a**[a]	258 (17300)
$[Ag_2(\mu\text{-dcpm})_2][Ag(CN)_2]_2$, **3b**[a]	257 (18000)
$[\{(Cy_3P)Cu(CN)\}_3]_\infty$, **4**[b]	236 (44000), 246 (sh, 27600), 270 (sh, 4240)
$[Cu_2(\mu\text{-dcpm})_2(CN)_2]$, **5**[b]	276 (17600)
$[\{Cu(dcpe)\}_2(CN)(\mu\text{-dcpe})]PF_6$, **6**($PF_6$)[b]	239 (78000), 280 (sh, 2500), 349 (560)
$[\{Cu(dppp)\}_3(CN)_2(\mu\text{-dppp})]PF_6$, **7**($PF_6$)[b]	272 (57800)
$[Cu(CN)(PCy_3)]_6$, **8**[b]	247 (sh, 40400), 282 (sh, 2930)

[a] In acetonitrile. [b] In dichloromethane.

Electronic Absorption Spectroscopy. The UV−visible spectra of **1** and **2** in acetonitrile are depicted in Figure 9, and the spectral data are listed in Table 3. For **1**, a strong absorption band at 218 nm (ϵ = 7200 dm^3 mol^{-1} cm^{-1}) and a weak shoulder at 245 nm (ϵ = 350 dm^3 mol^{-1} cm^{-1}) are observed. An intense high-energy absorption band at λ_{max} = 203 nm with a shoulder at 216 nm (ϵ = 31 500 and 23 000 dm^3 mol^{-1} cm^{-1}, respectively) has also been observed for **2**. The profiles of the absorption spectra for **1** and **2** are similar to that of a dilute aqueous solution of $K[Ag(CN)_2]$ (5.0×10^{-4} mol dm^{-3}) as reported by Patterson and coworkers.[15] For the μ-dcpm bridged complexes **3a** and **3b**, intense absorption bands at λ_{max} = 258 (ϵ = 17 300 dm^3 mol^{-1} cm^{-1}) and 257 nm (ϵ = 18 000 dm^3 mol^{-1} cm^{-1}), respectively, are observed in CH_3CN, and they are comparable to the $^1[4d\sigma^* \rightarrow 5p\sigma]$ transition at 266 nm (ϵ = 22 000 dm^3 mol^{-1} cm^{-1}) previously reported for the $[Ag_2(dcpm)_2]^{2+}$ salts.[34]

Figure 10 depicts the absorption spectra of **4**, **5**, **6**, and **8** in dichloromethane at 298 K. The absorption spectrum of **4** exhibits a peak at λ_{max} = 236 nm (ϵ = 44 000 dm^3 mol^{-1} cm^{-1}) with weak and broad absorption tailing from 270 to 350 nm (ϵ = 4240−920 dm^3 mol^{-1} cm^{-1}). The absorption spectrum of **5** exhibits an intense absorption at λ_{max} = 276 nm, the ϵ value of which (17 600 dm^3 mol^{-1} cm^{-1}) is significantly higher than that of **4** at 270 nm (4240 dm^{3}mol^{-1}cm^{-1}). Our previous work on $[Cu_2(dmpm)_3]^{2+}$ shows that the $[3d\sigma^* \rightarrow 4p\sigma]$ transition of this compound

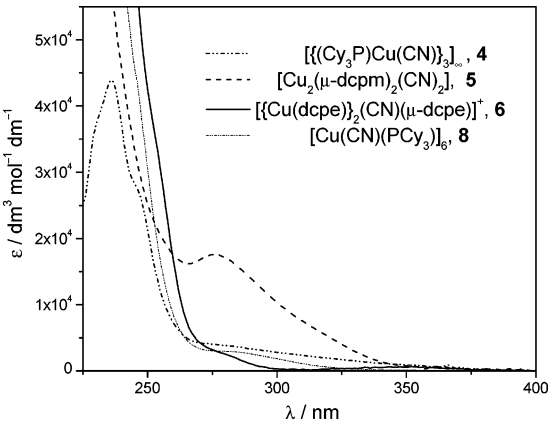

Figure 10. UV−vis absorption spectra of **4**, **5**, **6**, and **8** in dichloromethane at 298 K.

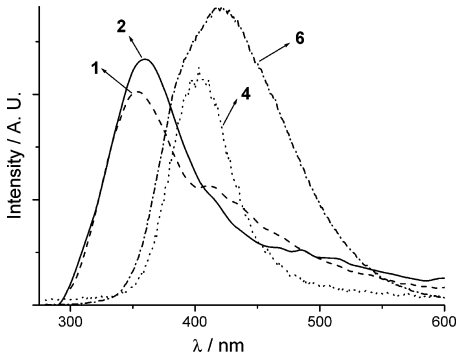

Figure 11. Room-temperature solid-state emission of **1**, **2**, **4**, and **6** (λ_{ex} = 250 nm).

occurs at λ_{max} = 276 nm (ϵ = 10 800 dm^3 mol^{-1} cm^{-1}) in H_2O,[37] which is similar to the 276-nm band of **5**. The absorption spectrum of **6** shows an intense band at λ_{max} = 239 nm (ϵ = 78 000 dm^{3}mol^{-1}cm^{-1}) and a weak shoulder at 280 nm (ϵ = 2500 dm^3 mol^{-1} cm^{-1}), whereas that of **8** exhibits a weak absorption tail from 282 to 326 nm (ϵ = 2930−370 dm^3 mol^{-1} cm^{-1}). Such weak absorption in the 265−350-nm spectral region for **8** is comparable to that observed for **4** and is consistent with the absence of close intramolecular metal−metal interactions. For **7**, the 272-nm absorption band with a large ϵ value of 57 800 dm^3 mol^{-1} cm^{-1} is slightly red-shifted from the 252-nm absorption (ϵ = 15 000 dm^3 mol^{-1} cm^{-1}) of the free dppp ligand, which can be assigned to be mainly contributed by intraligand transition of the dppp ligand.

Solution- and Solid-State Emission Spectroscopy. Emission data for **1**−**8** are listed in Table 4. Complexes **1** and **2** are nonemissive at 298 K in CH_3CN, whereas **3a** and **3b** show weak luminescence at λ_{max} = 365 nm in CH_3CN at 298 K with a quantum yield of ∼6 × 10^{-3} and lifetime of ∼0.2 μs. In MeOH/EtOH (1:4) glass at 77 K, **1** and **2** exhibit an intense emission at λ_{max} = 397 and 391 nm with lifetime of 268 and 320 μs, respectively. The excitation spectrum of **1** (concentration = 1.0 × 10^{-3} M) in glassy MeOH/EtOH (1:4) solution exhibits a peak at 238 nm, which is similar to the 250-nm excitation band for the 390-nm emission of K[Ag(CN)$_2$] in frozen (77 K) aqueous solution at the same complex concentration.[15] A 77 K MeOH/EtOH (1:4) glassy solution of **3a** or **3b** shows an intense, broad emission at λ_{max} = 360 nm with a lifetime of ∼45 μs. An additional peak at 412 nm was also found in the spectrum of **3a**. The emission lifetimes of **1**−**3a,b** recorded in 77 K glassy solutions are significantly longer compared to those recorded in acetonitrile at 298 K, revealing a large temperature dependence of the emission lifetimes. The room-temperature solid-state emission spectra of **1**−**3a,b** exhibit peaks at λ_{max} = 356−408 nm (Figure 11). At 77 K, the solid-state emission of **1** occurs at λ_{max} = 366 nm, whereas those of **2**−**3a,b** are at 347−382 nm. The emission quantum yields and lifetimes of solid samples of **1**−**3a,b** measured at 298 K are (2.3−8.0) × 10^{-3} and 0.6−87 μs, respectively.

Complexes **4**−**6** and **8** are nonemissive in CH_2Cl_2 or CH_3CN, whereas **7** is weakly emissive with λ_{max} = 445 nm in dichloromethane at 298 K. In MeOH/EtOH (1:4) glass at 77 K, **4**−**8** display intense emission at λ_{max} = 382−416 nm. A weak, broad emission with λ_{max} = 500 and 549 nm was recorded for MeOH/EtOH glassy solutions of **5** and **6**, respectively. These visible emissions are comparable in energy with that of [Cu(dcpm)$_2$](PF$_6$)$_2$ (λ_{max} = 506 nm) and [Cu$_2$(dmpm)$_3$](ClO$_4$)$_2$ (λ_{max} = 521 nm) recorded under similar conditions[37] and are attributed to originate from the ^{3}[(3d$_{x^2-y^2}$, d$_{xy}$)^1(4p$_z$)^1] excited state of a Cu(I) site. Complex **4** exhibits an intense solid-state emission at λ_{max} = 401 (ϕ_o = 2.0 × 10^{-3}) and 405 nm at 298 (Figure 11) and 77 K, respectively, and there is a significant temperature dependence of the emission lifetime [τ = 1.0 μs at 298 K to 109 μs at 77 K]. The solid-state emission of **5** with λ_{max} at 470 nm (298 K) and 488 nm (77 K) are red-shifted from those observed for **4** (401 nm at 298 K; 405 nm at 77 K), but they are comparable to the solid-state emission of [Cu$_2$(dcpm)$_2$]X$_2$

Table 4. Emission Data of Complexes **1**−**8** (λ_{ex} = 250 nm)

	solid state		fluid (concentration 5 × 10^{-4} M)	
	298 K λ_{max}/nm; ϕ_o; τ_o/μs	77 K λ_{max}/nm (τ_o/μs)	298 K λ_{max}/nm; ϕ_o; τ_o/μs	77 K[c] λ_{max}/nm (τ_o/μs)
[(Cy$_3$P)Ag(NCAgCN)]$_\infty$, **1**	356; 8.0 × 10^{-3}; 5.4	366 (50)	nonemissive[a]	397 (268)
[(Cy$_3$P)$_2$Ag(NCAgCN)], **2**	360; 6.5 × 10^{-3}; 0.6	347 (58)	nonemissive[a]	391 (320)
[Ag$_2$(μ-dcpm)$_2$][Ag(CN)$_2$]$_2$·(CH$_3$OH)$_2$, **3a**·(CH$_3$OH)$_2$	408; 2.3 × 10^{-3}; 87	381 (55)	365; 6.1 × 10^{-3}; 0.26[a]	360 (max, 48), 412 (535)
[Ag$_2$(μ-dcpm)$_2$][Ag(CN)$_2$]$_2$, **3b**	395; 3.7 × 10^{-3}; 31	382 (58)	365; 6.7 × 10^{-3}; 0.20[a]	360 (43)
[{(Cy$_3$P)Cu(CN)}$_3$]$_\infty$, **4**	401; 2.0 × 10^{-3}; 1.0	405 (109)	nonemissive[b]	400 (130)
[Cu$_2$(μ-dcpm)$_2$(CN)$_2$], **5**	470; 8.0 × 10^{-2}; 28	488 (123)	nonemissive[b]	382 (max, 60), 500 (sh, 341)
[{Cu(dcpe)}$_2$(CN)(μ-dcpe)]PF$_6$, **6**(PF$_6$)	422; 4.9 × 10^{-3}; 4.8	408 (204)	nonemissive[b]	416 (max, 320), 549 (298)
[{Cu(dppp)}$_3$(CN)$_2$(μ-dppp)]PF$_6$, **7**(PF$_6$)	462; 6.8 × 10^{-3}; 3.7	462 (430)	445; 1.76 × 10^{-3}; 0.30[b]	405 (1370)
[Cu(CN)(PCy$_3$)]$_6$, **8**	415; 3.0 × 10^{-3}; 2.0	410 (86)	nonemissive[b]	405 (96)

[a] In CH_3CN. [b] In CH_2Cl_2. [c] In EtOH/MeOH (4:1).

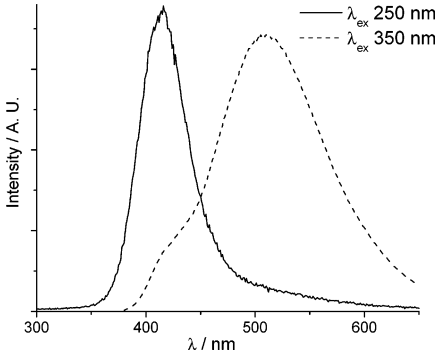

Figure 12. Room-temperature solid-state emission of **8** (λ_{ex} = 250 and 350 nm).

(X = ClO_4^-, PF_6^-, I^-) with emission maxima at 460−475 nm at 298 K, respectively.[37] When solid samples of **6** and **8** (Figures 11, 12) are excited at 250 nm, a broad structureless emission at 408−422 nm appears, which is similar in energy to that observed for **4** (Figure 11). Upon excitation of a crystalline sample of **8** at 350 nm, a broad emission with λ_{max} at 510 nm (Figure 12) and 506 nm was observed at 298 and 77 K, respectively. The change in solid-state emission energy of **8** with the excitation energy indicates that the emissions may originate from multiple sites. The solid-state emission of **7** (λ_{max} = 462 nm) at 298 K is red-shifted from the 423-nm emission of the solid dppp. We assign the former to come from a $^3[(3d_{x^2-y^2}, 3d_{xy})(4p_z)]$ excited state of a three-coordinate Cu(I) site, although mixing with an intraligand triplet excited state of dppp could not be excluded. The solid-state emission quantum yields of **4** and **6**−**8** lie between 2.0 × 10^{-3} and 6.8 × 10^{-3}, whereas that of **5** exhibits a comparatively higher quantum yield of 8.0 × 10^{-2}.

Solutions of **3a** and **8** in CH_3OH and CH_2Cl_2, respectively, were used for preparation of thin films supported on glass slides to investigate the response to organic vapors.[39] Methanol, chloroform, acetone, acetonitrile, and ethanol vapors were produced by the diffusion tube method.[40] The N_2 gas containing the organic vapor was fed into a flow cell in which the film was exposed to the gas stream, and the glass slide was oriented to face the excitation light source in the luminescence spectrometer (Perkin−Elmer LS-50B). However, no emission response toward these volatile organic compounds was detected.

Discussion

General Remarks. As described for the copper(I) cyanodiimine system,[41] subtle changes in reaction conditions can lead to profound variations in products. In this work, reactions were undertaken in different stoichiometric ratios of the reactants, giving compounds with various coordination modes, geometries, and component stoichiometries. The $[Ag(CN)_2]^-$ moiety can act as an isolated counterion, a terminal ligand via one cyano group, or a bridging spacer, and this can afford compounds with diverse structures and dimensionalities. Reaction of PCy_3 with AgCN afforded the polymer $[(Cy_3P)Ag(NCAgCN)]_\infty$ (**1**), bearing AgCN to PCy_3 in a 2:1 ratio. The structure of **1** is similar to that described for the four-coordinate pyridine-solvated silver(I) polymer $[\{(o\text{-tolyl})_3P\}Ag(py)(NCAgCN)]_\infty$.[7] The $\{Ag(CN)\}_\infty$ backbone in **1** resembles that of the CuCN chain in $[Cu_4(CN)_4(2,2'\text{-biquinoline})]_\infty$.[42] However, in solution such as dichloromethane, the polymeric solid **1** is likely present as monomers or oligomers. The structure and stoichiometry of **2** are comparable to the repeating unit in the $[(Ph_3P)_2Ag(NCAgCN)]_\infty$ polymer.[7] The structures of **1** and **4** are similar; both have a zigzag polymeric configuration with a three-coordinate metal center coordinated by two cyanide groups and one PCy_3 unit. The difference is that the $[(Cy_3P)Ag]^+$ units in **1** are bridged by $[NCAgCN]^-$, whereas the $[(Cy_3P)Cu]^+$ groups in **4** are linked by a CN^- ligand. As for **1**, it is unlikely that solid **4** retains its polymeric structure. Complexes **3a** and **3b** with close intramolecular Ag···Ag distances could be viewed as models for weakly interacting AgCN units, and they show structural resemblance to the $[Ag_2(dcpm)_2]X_2$ complexes, the UV−visible absorption spectra of which show distinct [4dσ* → 5pσ] transition.[34] The molecular structures of **5**−**8** reveal negligible Cu···Cu contacts, although the Cu^I···CN^- interaction in **5** should not be overlooked in photophysical assignment (see below).

Absorption Energies. The high-energy intense absorption bands at λ = 203−218 nm (ε = (7.2 × 10^3)−(3.2 × 10^4) $dm^3\ mol^{-1}\ cm^{-1}$) for **1** and **2** are assigned to strongly allowed charge-transfer transitions, and similar transitions have been noted for the $[Ag(CN)_2]^-$ salts by Mason.[43] In the absorption spectrum of **1**, the lowest-energy band at λ_{max} = 245 nm with an extinction coefficient of 350 $dm^3\ mol^{-1}\ cm^{-1}$ signifies a forbidden transition (Figure 9). The intense absorption band of the μ-dcpm bridged complexes **3a** and **3b** in CH_3CN solution with λ_{max} at ∼257 nm (ε ≈ 1.8 × 10^4 $dm^3\ mol^{-1}\ cm^{-1}$) is in contrast with the absorption spectra of the mononuclear derivatives $[(Cy_3P)Ag(O_2CCF_3)]$ and $[Ag(PR_3)_2]ClO_4$ (R = Me, Cy), while the latter show ε values below 10^2 at λ ≥ 250 nm. The high ε values for the 257-nm absorption band of **3a** and **3b** are comparable to those for the [4dσ* → 5pσ] transition observed at λ_{max} = 266 nm (ε = 22000 $dm^3\ mol^{-1}\ cm^{-1}$) for the related $[Ag_2(\mu\text{-dcpm})_2]X_2$ (X = $CF_3SO_3^-$ and PF_6^-),[34] the spectroscopic assignment of which was supported by resonance Raman experiments. Therefore, the absorption bands of **3a** and **3b** at λ_{max} ≈ 257 nm are assigned to the ^{1}[4dσ* → 5pσ] transition.

The high-energy absorptions of **4** at λ < 250 nm show substantial extinction coefficients of (2.8−4.4) × 10^4 $dm^3\ mol^{-1}\ cm^{-1}$, which are comparable to that observed for $[Cu(CN)_2]^-$,[44] and these are assigned to charge-transfer absorptions. The less intense absorption shoulder tailing from 270 (ε = 4240 $dm^3\ mol^{-1}\ cm^{-1}$) to 300 nm (ε = 1360 dm^3

(39) Lu, W.; Chan, M. C. W.; Zhu, N.; Che, C.-M.; He, Z.; Wong, K.-Y. *Chem.—Eur. J.* **2003**, *9*, 6155−6166.
(40) Altshuller, A. P.; Cohen, I. R. *Anal. Chem.* **1960**, *32*, 802−810.
(41) (a) Chesnut, D. J.; Kusnetzow, A.; Birge, R.; Zubieta, J. *Inorg. Chem.* **1999**, *38*, 5484−5494. (b) Chesnut, D. J.; Plewak, D.; Zubieta, J. *J. Chem. Soc., Dalton Trans.* **2001**, 2567−2580.
(42) Chesnut, D. J.; Zubieta, J. *Chem. Commun.* **1998**, 1707−1708.
(43) (a) Mason, W. R. *J. Am. Chem. Soc.* **1973**, *95*, 3573−3581. (b) Mason, W. R. *J. Am. Chem. Soc.* **1976**, *98*, 5182−5187.
(44) Horváth, A.; Zsilák, Z.; Papp, S. *J. Photochem. Photobiol., A* **1989**, *50*, 129−139.

mol^{-1} cm^{-1}) is tentatively assigned to metal-centered [3d → (4p, 4s)] transition (Figure 10). For **5**, the intense absorption band with λ_{max} at 276 nm and ϵ value of 17 600 dm^3 mol^{-1} cm^{-1} resembles the metal−metal-bonded $^1[3d\sigma^* \rightarrow 4p\sigma]$ transitions of $[Cu_2(dmpm)_3]^{2+}$ at λ_{max} = 276 nm (ϵ = 10 800 dm^3 mol^{-1} cm^{-1}) in H_2O[37] and $[Cu_2(dcpm)_2]X_2$ ($X = ClO_4^-$, PF_6^-)[14c] at λ_{max} = 307−311 nm ($\epsilon \approx$ 15 000 dm^3 mol^{-1} cm^{-1}) in CH_2Cl_2. Thus, we similarly assign this absorption to a $^1[3d\sigma^* \rightarrow 4p\sigma]$ transition (or 3d → (4p, 4s) modified by Cu(I)−Cu(I) interaction). Complex **5** can be regarded as two weakly interacting CuCN units via Cu··· Cu contacts. The absorption spectra of **6** and **8** do not reveal a distinct absorption peak at $\lambda > 270$ nm that could be assigned to the $[3d\sigma^* \rightarrow 4p\sigma]$ transition. Rather, these two complexes show a broad absorption tailing from λ = 270 nm (ϵ = 3390−4320 dm^3 mol^{-1} cm^{-1}) to 300−325 nm ($\epsilon \approx$ 300−390 dm^3 mol^{-1} cm^{-1}, which are similar to that of **4** at 270 nm (ϵ = 4240 dm^3 mol^{-1} cm^{-1}). This is consistent with the structural data that the copper atoms in **6** and **8** are noninteracting (Figure 10).

Emission Energies. The near-UV solid-state luminescence of **1** and **2** at λ_{max} = 356−360 nm are assigned to originate from a metal-centered triplet excited state of a three-coordinate silver(I) site, and a tentative assignment would be the $^3[(4d_{x^2-y^2}, 4d_{xy}), 5p_z]$ excited state. For the binuclear complexes **3a** and **3b**, their solid-state emissions are slightly red-shifted from that observed for **1** and **2** and can be attributed to the formation of metal−metal-bonded exciplexes. Metal−metal-bonded exciplex formation has previously been proposed to account for the emission from $*[Ag(CN)_2^-]_n$ oligomeric sites in the doped crystals of dicyanoargentates(I).[16] For example, $[Ag(CN)_2]^-$ ions in a KCl host lattice at 77 K exhibit emission bands over the λ_{max} = 295−548-nm range upon excitation at different wavelengths (λ_{ex} = 226−315 nm). This was attributed to mono-, di-, tri-, and polymeric Ag(I) sites that emit at different wavelengths because of silver−silver-bonding interactions in both the ground and excited states. However, it should be noted that the Stokes' shifts ($\Delta\nu$) of the 298-K solid-state emission for **3a** (14 250 cm^{-1}) and **3b** (13 600 cm^{-1}) from their respective $^1(4d\sigma^* \rightarrow 5p\sigma)$ absorption bands at ∼258 nm in CH_3CN are larger than that reported for the related binuclear $[Au_2(dcpm)_2]^{2+}$ compound (8930 cm^{-1}).[14b] Thus, the origin of the emission from the **3a** and **3b** solids remains unclear. The small difference between the emission energies of **1** and **2** with those of **3a** and **3b** suggests that the impact of Ag(I)−Ag(I) interaction upon the emission of **3a** and **3b** is less important than previously envisaged.[34] The lifetimes in the microsecond range are consistent with the triplet excited-state assignment. The $^3[(4d_{x^2-y^2}, 4d_{xy}), 5p_z]$ excited state appears to play an important role in affecting the photoluminescence of these Ag(I) solids.

The 77 K glassy solution of **4**−**8** exhibit intense luminescence at λ_{max} = 382−416 nm. The solid-state emission of **5** [λ_{max} = 470 (298 K) and 488 nm (77 K)] is significantly red-shifted in energy from that observed for **4** [λ_{max} = 401 (298 K) and 405 nm (77 K)]. Referring to the room-temperature solid-state emission of $[Cu(PCy_3)_2]ClO_4$ at λ_{max} = 491 nm, an assignment of Cu−Cu-bonded excited state for the solid-state emission of **5** is precluded. We suggest that the interaction between the $[Cu_2(dcpm)_2]^{2+}$ core and CN^- could stabilize the excited state, which could lead to a lower-energy $^3[(3d_{x^2-y^2}, 3d_{xy}), 4p_z]$ excited state. Coordination of a halide ion to the excited $*[Cu(CN)_2]^-$ moiety in aqueous solution upon UV irradiation was previously observed to afford a highly luminescent exciplex with an emission band at 480 nm.[17a,44,45] This is similar in energy to the 470-nm emission of the $[Cu_2(dcpm)_2(CN)_2]$ solid (**5**). The solid-state emission of **8** at 298 and 77 K is dependent on the excitation wavelength; a red-shift of the emission maximum at 298 K was observed from 415 to 510 nm as the excitation wavelength increased from 250 to 350 nm. We propose that the six Cu(I) sites exhibit subtly different coordination environments within the hexagonal-like geometry of **8** in the solid state, and these environments respond to different excitation wavelengths and emit at slightly varying energies.[46] This is in accordance with a $^3[(3d_{x^2-y^2}, 3d_{xy}), 4p_z]$ emissive excited-state assignment.

In the literature, oligomerizations of $Ag(CN)_2^-$ and $Au(CN)_2^-$ ions in solution at high complex concentrations have been proposed, and these oligomerizations were manifested by red-shifted absorption and emission bands compared to monomer counterparts recorded in low-complex concentrations.[15] While the phenomenon of metal−metal-bonded exciplex formation could be invoked to rationalize the spectral data previously observed by Patterson and Fackler,[15,16] this may not be the only factor affecting the photoluminescence of $M(CN)_2^-$ solids. The similarity in energy between the emission of the three-coordinate complexes **1** and **2** and some of the high-energy emissions (λ_{max} = 327−345 nm) for the $[Ag(CN)_2^-]_n$ solid reported in the literature[16a] suggests that silver(I)-ligand coordination is crucial in affecting the emission energy. It is pertinent to note that monomeric three-coordinate Ag(I) and Cu(I) species bearing CN^- ancillary ligands exhibit near-UV photoluminescence at ∼360 and 400 nm, respectively, and the high-emission energy is consistent with the large $nd - [(n+1)(s, p)]$ band gap of Cu(I) and Ag(I).

It is interesting to note that the photoluminescence from these Ag(I)− and Cu(I)−cyanide solids can be intense and have long lifetimes. These photophysical features signify the potential applications of Ag(I)− and Cu(I)−CN solids as new classes of blue light-emitting materials. Although Ag(I)−Ag(I) and Cu(I)−Cu(I) interactions could modify the metal-centered [$nd \rightarrow (n+1)(p, s)$] transition energy, the effect of Ag(I)−Ag(I) interaction upon the photoluminescent energy can be latent, as revealed by the comparable emission energies of **1** and **2** relative to those of **3a** and **3b**.

Concluding Remarks

The employment of a sterically unencumbered $[Ag(CN)_2]^-$ building block has yielded, depending on the initial reactant

(45) (a) Horváth, A.; Papp, S.; Décsy, Z. *J. Photochem.* **1984**, *24*, 331−339. (b) Horváth, A.; Stevenson, K. L. *Inorg. Chim. Acta* **1991**, *186*, 61−66.
(46) Henary, M.; Zink, J. I. *Inorg. Chem.* **1991**, *30*, 3111−3112.

stoichiometry, a one-dimensional chain with alternate $[(Cy_3P)Ag]^+$ and $[Ag(CN)_2]^-$ units or a discrete $[(Cy_3P)_2Ag(NCAgCN)]$ molecule. Reactions of MCN (M = Ag(I), Cu(I)), or $[Cu(CH_3CN)_4]PF_6$ (with KCN) with bidentate $R_2P-(CH_2)_n-PR_2$ (R = Cy, n = 1−2; R = Ph, n = 3) phosphine ligands afforded a series of bi- and trinuclear macrocycles. Both metal−metal interaction and metal−ligand coordination have been observed to affect the photophysical properties of these M(I)−CN solids. The existence of M(I)−M(I) interaction in the excited state has been verified by the presence of an intense dipole-allowed, red-shifted absorption attributed to the [nd$\sigma^* \rightarrow (n+1)p\sigma$] transition, but the ^{3}[$(n+1)$pσ, ndσ^*] emission could not be assigned without ambiguity. The metal−ligand coordination in both ground and excited states leads to emission from the ^{3}[(nd$_{x^2-y^2}$, nd$_{xy}$), $(n+1)$p$_z$] state of a three-coordinate M(I) site. Interestingly, such emissions are found at comparable or lower energy than the expected ^{3}[$(n+1)$pσ, ndσ^*] emission of dinuclear Ag(I)− and Cu(I)−phosphine complexes, the latter would occur at energies in the UV region (λ < 400 nm). Thus, assignment of emission to a metal−metal-bonded excited state of Ag(I) and Cu(I) metal−cyanide complexes should be cautious, and metal−anion coordination at two-coordinate d^{10} metal site should be taken into consideration in the spectroscopic assignments of these systems.

Acknowledgment. We are grateful for financial support from The University of Hong Kong, HKU Large Item Equipment Grant, Research Grants Council of the Hong Kong SAR, China (HKU 7039/03P), and the National Natural Science Foundation of China/Research Grants Council Joint Research Scheme (N_HKU 742/04). We thank Dr. Kong-Hung Sze for helpful discussions on NMR spectroscopy.

Supporting Information Available: Listings of crystal data, atomic coordinates, calculated coordinates, anisotropic displacement parameters, and bond lengths and angles for **1**−**8** in CIF format; $^{31}P\{^1H\}$ NMR spectra of **7** in $CDCl_3$ at different temperature and $^{31}P-^{31}P$ COSY spectrum of **7** in CD_2Cl_2 at 25 °C. This material is available free of charge via the Internet at http://pub.acs.org.

IC048876K